A constitutively-active IKK-complex at the axon initial segment

Hans-Georg König[a,b,*], Orla Watters[a,b], Sinéad Kinsella[a,b,#], Mohammed Ameen[a], Beau J. Fenner[a,¶] and Jochen H. M. Prehn[a,b,*]

[a]Department of Physiology and Medical Physics, Royal College of Surgeons in Ireland, 123 Saint Stephen's Green, Dublin 2, Ireland); [b]Centre for the Study of Neurological Disorders, Royal College of Surgeons in Ireland, 123 Saint Stephen's Green, Dublin 2, Ireland; [#]Present address: Program in Immunology, Clinical Research Division, Fred Hutchinson Cancer Research Center, 1011 Fairview Avenue N.,Seattle, WA 98109, USA. [¶]Present address: Singapore National Eye Centre, 11 Third Hospital Avenue, Singapore 168751, Singapore.

Authors' e-mail: H.G.K: hgkoenig@rcsi.ie; O.W.: orlawatters@rcsi.ie; S.K.: sineadkinsella@rcsi.ie; M. A.: mohammedameen@rcsi.ie; B.F.: beaufenner@gmail.com; J.H.M.P.: prehn@rcsi.ie

***Corresponding authors:** HGK (hgkoenig@rcsi.ie) & JHMP (prehn@rcsi.ie); Tel.: + 353 1 402 2260; Fax.: +353 1 402 2447

Text pages: 31

Figures: 6

Number of words in the Abstract: 161

Number of words in the Introduction: 500

Number of words in the Results: 1361

Number of words in the Discussion: 987

Number of words in Experimental procedure: 1457

Number of words in Figure Legends: 1323

Abbreviations: AIS, axon initial segment; ASA, acetyl-salicylic acid; DMEM, Dulbecco's modified Eagle media; eGFP; enhanced green-fluorescent protein; FADD, Fas-associated death domain; FBS, fetal bovine serum; FGF, fibroblast growth factor; FSC, forward scatter; HBSS, Hanks' Balanced Salt solution; HS, horse serum; HRP, horseradish peroxidase; IGEPAL, Octylphenoxy poly(ethyleneoxy)ethanol, branched; IκBα, inhibitor of κB–α; IKK, IκB-kinase; IL-1, interleukin-1; JNK, c-Jun N-terminal kinases; KCNQ, delayed rectifier potassium channel, voltage-gated, KQT-like subfamily; MAPK, mitogen-activated protein kinase; MAPKK, mitogen-activated protein kinase kinase; NEMO, NF-κB essential modulator (IKKγ); NF-κB, Nuclear factor kappa-light-chain-enhancer of activated B cells; PC12 Phaeochromocytoma 12; PLA, proximity ligation assays; PIPES, 1,4-Piperazinediethanesulfonic acid; RPMI, Roswell Park Memorial Institute media; R-type calcium channel, resistant/residual opening calcium channels; Rel, retikuloendotheliosis; shRNA, small-hairpin RNA; SAPK, stress-activated protein kinases; SSC, sideward scatter; TNF-α, tumor necrosis factor-α; TRADD, tumor necrosis factor receptor type 1-associated death domain protein; T-type calcium channel, transient opening calcium channels

Abstract.

Background: Previous studies provided evidence for an accumulation of IκB-kinase (IKK) α/β at the axon initial segment (AIS), a neuronal compartment defined by ankyrin-G expression. Here we explored whether the presence of the IKK-complex at the AIS was associated with the activation of IKK signaling at this site. Methods and Results: Proximity-ligation assays (PLAs) using pan-IKKα/β, phospho-IKKα/β-specific as well as ankyrin-G specific antibodies validated their binding to proximal epitopes in the AIS, while antibodies to other phosphorylated signaling proteins showed no preference for the AIS. Small-hairpin mediated silencing of IKKβ significantly reduced anti-phospho-IKKα/β-immunoreactivities in the AIS. *ank3* gene-deficient cerebellar Purkinje cells also exhibited no phosphorylated IKKα/β at the proximal region of their axons. Transient ankyrin-G overexpression in PC12 cells augmented NF-κB transactivation in an ankyrin-G death-domain dependent manner. Finally, small molecule inhibitors of IKK-activity, including Aspirin, inhibited the accumulation of activated IKK proteins in the AIS. Conclusion: Our data suggest the existence of a constitutively-active IKK signaling complex in the AIS.

Keywords: axon initial segment; NF-κB; IKK 2 Kinase; ankyrin-G; proximity ligation assay; axon

1. Introduction.

In the central nervous system, the transcription factor nuclear factor-κB (NF-κB) is regularly composed of p50, p65/RelA and c-Rel-containing heterodimers. Inactive NF-κB is sequestered in the cytosol by association with its inhibitor of κB (IκBα) (Chen et al., 1995). Phosphorylation of IκBα by the inhibitor of κB-kinase (IKK)-complex results in the degradation of the protein and liberation of NF-κB for translocation into the nucleus (Zandi et al., 1998). IKKα/β occurs as heterodimers or homodimers and associates with IKKγ to compose the IKK signalosome. Autophosphorylation of IKKα/β within its activation domain, resulting in the phosphorylation of Ser177/181 of human IKKβ and Ser176/180 of human IKKα, have been suggested as essential in their activation mechanism (Mercurio et al., 1997) (Zandi et al., 1997). NF-κB is constitutively active in the CNS (Kaltschmidt et al., 1994) and inducible in response to neuronal activity (Meffert et al., 2003) as well as cytokine treatment (Bui et al., 2001). NF-κB drives the transcription of a wide range of target genes in neurons, such as pro-survival genes (Bui et al., 2001), neuronal adhesion molecules (Simpson and Morris, 2000), proteins regulating synaptogenesis and synaptic maturation (Schmeisser et al., 2012) and cytoskeletal anchor proteins including ankyrin-G (Konig et al., 2017).

Ankyrin-G is essential for the assembly and maintenance of the axon initial segment (AIS)(Freal et al., 2016), a neuronal compartment that in most neurons is required to convert synaptic input into action potential generation (Baranauskas et al., 2013; Kole et al., 2008). Ankyrin-G sequesters ion channels including the sodium channels $NaV_{1.2}$ (Brachet et al., 2010) and $NaV_{1.6}$ (Gasser et al., 2012), and the M-current potassium channels KCNQ2/3 (Rasmussen et al., 2007). Voltage-gated T and

R-type calcium-channels co-localize with sodium channels in the AIS and modulate spike frequency and timing (Bender and Trussell, 2009). Fibroblast-growth factor homologous factors, FGF12-14 are intracellular proteins that regulate sodium-channel activity at the AIS (Lou et al., 2005; Wildburger et al., 2015).

Others and we had previously described that immunoreactivity against the upstream kinase of NF-κB, IKKα/β, could be found at the AIS and at the nodes of Ranvier in neurons at rest (Politi et al., 2008; Sanchez-Ponce et al., 2008; Schultz et al., 2006). In subsequent studies, pan-p65, pan-IKKα/β (Konig et al., 2017) as well as pan-NEMO immunoreactivity (Konig et al., 2012; Konig et al., 2017) were also found at the AIS following detergent extraction, a method used to carefully remove proteins that are not associated with the cytoskeleton. However a single previous report also demonstrated that immunoreactivity against the phosphorylated IκBα protein at the AIS persisted in IκBα gene-deficient mice (Buffington et al., 2012), questioning the presence of NF-κB signaling components at the AIS.

Using proximity-ligation assays, small-hairpin mediated gene silencing, gene deficient mice and pharmacological approaches, we here set out to investigate whether phosphorylated components of the NF-κB cascade localize to the AIS, and whether IKK activity is required for the accumulation of active, phosphorylated p65 at the AIS. Our data suggest the presence of a constitutively-active IKK signaling complex in the AIS.

2. Results.

2.1 Multiple anti-phosphorylated IKKα/β-antibodies label the AIS and their epitopes can be found in molecular proximity to AIS-bound pan-IKKα/β antibodies.

We had previously shown that IKK, the upstream kinase of IκBα, is present in the AIS (Konig et al., 2012; Konig et al., 2017). Using mature mouse cortical neurons, we found that significant anti-phosphorylated IKKα/β (pIKK) immunoreactivity was detectable in the AIS, demarcated by anti-ankyrin-G immunoreactivity (Fig 1A-F). Anti-phosphorylated IKKα/β (pIKK) immunolabeling was reduced by prolonged washes with ice-cold phosphate-buffered saline solution (data not shown), and required immediate fixation using pre-warmed, buffered formaldehyde solutions, suggesting that carefully optimized conditions during fixation are required to detect the activated kinase. To test whether different antibodies raised against the phosphorylated IKKα/β epitope were reactive in the AIS, we used anti phospho-Ser177/181 IKKβ (Ser176/180-IKKα) antibodies, as well as antibodies raised against anti-phospho-Ser181 IKKβ (Ser180 IKKα) only. Both types of antibodies were reactive in the AIS (Figure 1A&B), whereas antibodies raised against anti-phospho-Thr180/Tyr182 of p38α/MAPK14 or anti-phospho-Thr183/Tyr185 SAPK/JNK did not show enhanced immunolabeling in the AIS (Figure 1C&D). The latter kinases have been shown to be involved in axonal stress response pathways (Cavalli et al., 2005; Gerdts et al., 2011; Yang et al., 2015). Anti-phosphorylated IKKα/β immunoreactivities in the AIS were preserved following extraction of cytosolic proteins, however anti-phosphorylated SAPK/JNK immunoreactivities showed no AIS staining following detergent extraction (Figure 1E&F). As a further test for antibody-specificity, we employed proximity-ligation assays (PLA) between pan-

specific and phospho-specific IKKα/β antibodies. PLA-dots appear where both antibodies bind within ca. 40 nm from each other (Soderberg et al., 2007)(Schematic Figure 1G). Significantly more PLA-products were detected along the ankyrin-G-positive AIS and in the soma of neurons than in a comparable dendritic area (Figure 1H&I). These data suggested that anti-pan and anti-phosphorylated IKKα/β immunoreactivity bind to the same protein in the AIS.

2.2 IKKβ-silencing reduces anti-phosphorylated IKKα/β immunofluorescence intensities in the AIS.

We previously showed IKKβ protein presence at the AIS (Konig et al., 2017). To further substantiate our findings and to demonstrate antibody specificity, we employed small-hairpin constructs directed at IKKβ mRNA. To test the efficiency of four different small-hairpin vector constructs, we transfected murine Neuro-2A cells for four days with the relevant constructs. We also included cells transfected with an IKKβ expression plasmid as a positive control. IKKβ protein abundance was effectively diminished by IKKβ shRNA sequences 'A' and 'C' (Figure 2A,B). We then performed small-hairpin RNA-mediated silencing of IKKβ for 4 days in mature cortical neurons with eGFP (enhanced green fluorescent protein) expressed from the same plasmid. Following immunolabeling using anti-phosphorylated IKKα/β antibodies, we detected a decreased immunoreactivity along the AIS in cells transfected with IKKβ 'A' and 'C' small-hairpin constructs (Figure 2C,D). The mean (and median) area under the curve of pIKKα/β immunofluorescence along the AIS was strongly decreased by co-transfection of IKKβ 'A' and 'C' shRNAs from 65.80 ± 2.93 by 12.37 ± 3.22 (n = 225-239 cells per group, p=0.0003; by 9.72 ± 3.64 for 'C').

The decreased cellular IKKβ protein abundance thus reduced IKKβ levels at the AIS and hence immunofluorescence intensity using phosphorylation-specific antibodies.

2.3 Phosphorylated IKK co-localizes and interacts with ankyrin-G in vitro and in vivo.

We next investigated whether ankyrin-G and phosphorylated Ser176/177&180/181-IKKα/β immunoreactivities co-localized along the proximal axon of neurons. We stained mature cortical neurons with anti-phosphorylated IKKα/β and ankyrin-G specific antibodies, and plotted the normalized immunofluorescence intensities of ankyrin-G and phosphorylated IKKα/β along the AIS against each other. Co-localization of the highest pixel intensities for the pIKKα/β and ankyrin-G staining was found in a punctate pattern along the AIS suggesting the proteins co-localized in vesicular compartments along the AIS (Figure 3A&B). Anti-phosphorylated IKKα/β and anti-ankyrin-G immunoreactivity intensities correlated along the ankyrin-G positive AIS stretch, only minimally deviating from an ideal correlation (dotted line) of pixel intensities (Figure 3C). Next, we examined whether expression levels and localization during axonal development *in vitro* concurred to provide evidence in support of a co-developmental pattern. We found that phosphorylated IKKα/β and ankyrin-G immunoreactivities increased in parallel at the AIS during development from DIV4 to DIV18 (Figure 3D). Of note, we observed the co-clustering of ankyrin-G and phospho-IKKα/β immunoreactivities in brain slices derived from the cerebral cortex following immediate and mild brain fixation *in vivo* (Figure 3E). To further analyze whether anti-phospho-IKKα/β were found in molecular proximity (≲40 nm) to ankyrin-G epitopes, we employed proximity-ligation assays (PLA, Schematic Figure 4A). We found that PLA spots

densely clustered along proximal axons, indicating molecular proximity between phosphorylated-IKKα/β and ankyrin-G *in situ*, and they occurred in significantly higher numbers along the AIS than within the somatic compartment (Figure 4B-D). We next examined whether *ank3*/ankyrin-G gene knockout ablated IKK-phosphorylation in the AIS. Mice with a cerebellar-specific knockout of ankyrin-G were deficient in phosphorylated IKKα/β at the proximal region of cerebellar Purkinje cell axons (Figure 4E).

2.4 Ankyrin-G overexpression increases IKK-phosphorylation levels and NF-κB activity in a death-domain dependent fashion in cells devoid of an AIS.

In further immunolabeling studies, we found AIS immunoreactivity for two downstream targets of IKKα/β kinase activity in the AIS [see also (Pradere et al., 2016; Sakurai et al., 2003; Zandi et al., 1998)]. Immunoreactivity against phosphorylated p65 and phosphorylated IκBα could be detected in the AIS using mouse monoclonal antibodies (clone 7F1) directed at Ser536 of p65 (Ser534 in mouse p65) and (clone 5A5) directed at Ser32/36-phosphorylated IκBα (Figure 5A&B), further suggesting the existence of a constitutively-active IKK-complex at the AIS. We took two different experimental approaches to test this hypothesis. In a first approach, we performed experiments in neuronal-like phaeochromocytoma-cell line 12 (PC12) cells that are devoid of an AIS. Here, we explored whether ectopic Ankyrin-G expression was sufficient to activate IKK signaling. Ankyrin-G isoforms of 190, 270 and 480 kDa length are found at the AIS. The 480 kDa variant, bearing a long, neuron-specific tail-domain is indispensable for the accumulation of the two other isoforms of this scaffolding protein at this site (Freal et al., 2016). We tested whether increased IKK-phosphorylation could be induced by ectopic ankyrin-G

expression of the 270 kDa isoform in PC12 cells. Cells were transfected with increasing levels of ankyrin-G expression vectors together with or without plasmids encoding IKKβ. We found that higher ankyrin-G levels coincided with higher levels of phosphorylated IKKα/β. This was accompanied by increased levels of phospho-Ser32,36-IκBα and phospho-Ser536-p65, both downstream targets of the IKK-kinase (Figure 5C). In flow cytometry analyses we furthermore assessed how anti-phospho IKKα/β immunoreactivity was affected by co-transfection of both plasmids. More PC12 cells had high anti-phospho-IKKα/β immunoreactivity following ankyrin-G-eGFP and IKKβ-plasmid co-expression compared to cells expressing ankyrin-G-eGFP constructs only (Figure 5D). Similarly, when co-expressed in mature cortical neurons, we found that overexpression of both plasmids resulted in an increased immunoreactivity against Ser536-p65 in the AIS compared to IKKβ-only or control-transfected cells (Figure 5E). We then silenced ankyrin-G transiently for one day in PC12 cells and noticed a significant reduction of NF-κB transactivation potential (Figure 5G). Transiently overexpressing ankyrin-G in PC12 cells for one day increased NF-κB activity (Figure 5F,H,I). This rise was partly dependent on the death-domain of 270 kDa ankyrin-G, as we observed reduced activity following transfection of a death-domain deficient ankyrin-G plasmid (Figure 5F,I). We then built a vector expressing the sequence of the isolated death-domain of ankyrin-G. Following overexpression in PC12 cells for one day, cells with the highest amount of transfected plasmid showed numerically increased NF-κB reporter gene activity (Figure 5J).

2.5 Aspirin and other IKK-inhibitors effectively decrease phosphorylated IKK accumulation at the AIS.

In a second approach, we tested whether IKK phosphorylation levels were attenuated by IKK inhibitors, including BMS-3435541, an allosteric inhibitor of IKKβ and α (Burke et al., 2003), IKK-inhibitor VII, an ATP-competitive inhibitor of the IKKs, Bay11-7082, a MyD88-dependent inhibitor of IKK activation (Strickson et al., 2013) and manumycin, a farnesyltransferase inhibitor that also affects IKK-phosphorylation. Addition of each of the four inhibitors to mature cultured cortical neurons dose-dependently decreased anti-phosphorylated-IKKα/β immunofluorescence intensities at the AIS within hours (Figure 6A&B). Additionally, we used acetylsalicylic acid (ASA, Aspirin®), an inhibitor of IKKβ at physiological concentrations *in vitro* and *in vivo* (Grilli et al., 1996; Yin et al., 1998). ASA significantly decreased phospho-IKKα/β immunofluorescence along the AIS in a dose-dependent manner (Figure 6C-D).

3. Discussion.

We here characterized the accumulation of activation-loop phosphorylated IKKβ and pharmacological ablation of its constitutive phosphorylation in the AIS in primary neurons. We found that antibodies to IKK and ankyrin-G bound in close proximity to phosphorylated IKK within the AIS and determined that small-hairpin mediated silencing and IKK inhibitors induced a significant reduction of phosphorylated IKKα/β immunoreactivity in the AIS.

In the present study, we demonstrate that activated IKK is constitutively expressed in the AIS of mouse cortical neurons. We demonstrate that gene-silencing of IKKβ following transient transfection of primary neurons resulted in a significant decrease in anti-phosphorylated IKKα/β immunoreactivity in the AIS. The mild, transient gene silencing strategy over four days in matured neurons ensured that the AIS could develop normally, but that IKKβ phosphorylation levels were diminished in the differentiated AIS. Previous studies demonstrated pan-IKKα/β and pan-NEMO immunoreactivity localized to the AIS (Konig et al., 2012; Konig et al., 2017), and their immunostaining was found in clusters reminiscent of those previously found during IL-1 and TNF-α stimulation (Tarantino et al., 2014). Thus all three members of the IKK-signalosome are present at the AIS. Immunoreactivity against phosphorylated IκBα in the AIS, the subject of an earlier controversy, was previously demonstrated in neurons (Sanchez-Ponce et al., 2008; Schultz et al., 2006). Control experiments included enhanced anti-phosphorylated IκBα immunoreactivity using IκBα phospho-mimetic mutants, and abolished phosphorylated IκBα immunoreactivity after pre-treatment of the tissue with alkaline phosphatase (Schultz et al., 2006). Immunoreactivity against phosphorylated IκBα in the AIS was,

however, preserved in a mouse model with a targeted deletion of the full IκBα (*nfkbia*$^{-/-}$) locus (Beg et al., 1995; Buffington et al., 2012). The authors of the latter study suggested that anti-phosphorylated IκBα antibodies decorate an unrelated phosphoprotein in the AIS, as phosphorylation-specific antibodies can be promiscuous and the AIS may contain high amounts of phospho-proteins. Indeed, a previous proteomic study identified roughly 2000 phosphopeptides in neurons (Yu et al., 2013). To address the proposed promiscuous nature of the AIS in terms of phospho-proteins, we also demonstrated that neither phospho-p38, nor phospho-JNK immunoreactivity were enriched in the AIS. Similar to the IKK-complex, both of these kinases can be activated by MAPKK activity that is induced by stress-stimuli, and share common upstream regulatory kinases, including TAK with IKK (Wang et al., 2001). Of note, we also detected the downstream target of the IκB-kinase, Serine536-phosphorylated p65 in the AIS. Our study also demonstrated that pan-IKKα/β and phosphorylated IKK were in direct molecular proximity. Hence while the current study cannot fully resolve the controversy regarding the presence of phosphorylated IκBα immunoreactivity at the AIS, our data and data from other groups clearly demonstrate the presence of a phosphorylated IKK-complex and other key NF-κB signal transduction pathway proteins (IKKγ/NEMO, p65) at this site. We also observed that phosphorylated IKKα/β and ankyrin-G co-localized during *in vitro* development, and were in molecular proximity to each other in the soma and the initial segment. Previous studies not only found that IKK activity was essential for axon formation (Emmanouil et al., 2009; Sanchez-Ponce et al., 2008), but also that genetic silencing of IKKβ was sufficient to delay axon degeneration (Gerdts et al., 2011). Collectively, these findings suggest that IKKα/β and ankyrin-G interactions are essential for axon physiology and pathology.

Increased expression levels of ankyrin-G and IKKβ resulted in increased phosphorylation of the IKK-complex and its downstream targets p65 and IκBα. Notably, ankyrin-G isoforms expressed at the AIS contain a death-domain (DD) in their C-terminal tail (Del Rio et al., 2004; Zhang and Bennett, 1998), which may facilitate recruitment of adapter molecules such as tumor necrosis factor receptor type 1-associated death domain protein (TRADD) or Fas-associated death domain (FADD) (Lavrik et al., 2005), thus enabling activation of ubiquitin ligases and downstream IKK-complex activation. Indeed we found that transient, short-term overexpression of ankyrin-G moderately increased NF-κB activity in PC12 cells in a manner that depended on the expression of the death-domain of ankyrin-G. Our findings hence suggest that the C-terminal death domain of ankyrin-G is implicated in the phosphorylation of the IKK-complex. We previously also found that the p65/NF-κB transcription factor controls constitutive ankyrin-G expression levels in primary neurons (Konig et al., 2017). While short-term expression of ankyrin-G in PC12 cells augmented NF-κB activity, we had previously observed that longer expression in primary neurons diminished the transactivating potential of NF-κB, demonstrating that the transcription factor controls ankyrin-G expression in a negative feedback-loop in neurons (Konig et al., 2017). Our earlier study and the findings from the current study propose the concept that constitutive NF-κB activity during *in vitro* development is first induced and then restrained by ankyrin-G expression, possibly in a succession of positive and negative feedback loops, because an intricate balance of IKK-activity is required for physiological axon and initial segment formation.

We also found that pharmacological inhibition of IKK resulted in decreased IKK-phosphorylation levels at the AIS. Importantly, these results suggest that the NF-κB pathway in the AIS may represent a target for pharmacological intervention. It may be

possible to reinstate physiological ankyrin-G expression levels by modulating IKK-complex activity at the AIS. For example, painful neuromas are associated with increased ankyrin-G and sodium-channel expression levels (Kretschmer et al., 2004). Acetylsalicylic acid inhibits IKKα/β (Grilli et al., 1996; Yin et al., 1998), and this inhibition occurs in a dose-range consistent with serum levels observed after administration of therapeutic, analgesic doses (Feldman and Cryer, 1999). Interestingly, salicylates also show pronounced CNS toxicity following chronic administration to children (Gaudreault et al., 1982) which could be linked to effects on ankyrin-G expression.

In summary, our data demonstrate the presence of an activated, phosphorylated IKK-kinase in the AIS of neurons, and demonstrate that IKK activation leads to the accumulation of downstream NF-κB signaling molecules at the AIS. We also demonstrate that the popular non-steroidal anti-inflammatory drug acetylsalicylic acid (Aspirin®) reduces IKK-phosphorylation in the AIS, an effect that may contribute to its peripheral analgesic and potentially neurotoxic effects.

4. Experimental Procedure

4.1 Chemicals and Reagents. Chemicals were purchased from Sigma-Aldrich (Wicklow, Ireland) unless stated otherwise. Aspirin (ASA) was purchased from Sigma and Bayer (Leverkusen, Germany). Cell culture media and supplements were obtained from Gibco-Invitrogen (Dun Laoghaire, Ireland).

4.2 Cell culture and dual-luciferase assays. Neuro-2A cells were cultured in 50% RPMI, 50% Opti-MEM, and including 5% Fetal Bovine Serum (FBS), 2 mM L-Glutamine and 1% Penicillin/Streptomycin. Phaeochromocytoma (PC) 12 cells were cultured in RPMI media supplemented with 10% Horse Serum (HS), 5% FBS, 2 mM L-Glutamine and 1% Penicillin Streptomycin. Cells were kept in tissue culture incubators with a humidified atmosphere of 37 ºC and 5% CO_2. Cells were passaged every 3-4 days. PC12 and Neuro-2A cells were transfected using Lipofectamine 2000 (Gibco-Invitrogen) and Roche HP reagent (Sigma) using standard manufacturer protocols. Following hysterectomy, E16 *C57BL/6* mouse embryos were obtained and their cerebral cortices separated from meninges, minced, homogenized and trypsin-digested for 20-30 min at 37 ºC. The cortical cell suspension was plated at ca. 300,000 cells per cm^2 in DMEM, 10% FBS, 2 mM Glutamine and 1% Penicillin/Streptomycin for one day. Subsequently the neurons were grown in Neurobasal (Gibco), 2% B27, 1% GlutaMAX (Gibco), or NMEM-B27 media (1xMEM, 1 mM sodium pyruvate, 26 mM $NaHCO_3$, 2 mM GlutaMAX, 2% B27 and 33 mM β-D-Glucose), including β-D-arabino-furanoside (0.6 μM, days-in-vitro (DIV) 1-3). Transfection of primary neurons was conducted using calcium precipitation as previously described at ambient CO_2 levels for 2-4 hours (Goetze et al., 2003). Enhanced transfection rates were achieved by plate centrifugation at 1,500 rpm followed by incubation for 30 minutes prior to dissolving the complexes in HBSS, 33 mM β-D-glucose, 1 mM pyruvate and

15 mM HEPES. Transfections were conducted on Neuro-2A, PC12 cells or mature cortical neurons using pFlag-IKK-2 (IKKβ Addgene #11103), IKKβ-directed small-hairpin RNA plasmids that were purchased from Origene (Rockville, MD, USA, TG509787'A'-'D') or pAnkG-eGFP (270 kDa; a kind gift from V. Bennett, Duke University Medical Center, Durham, NC, USA), AnkG shRNA (Konig et al., 2012) as well as an eGFP vector. PC12 cells were transfected with NF-κB-response element firefly luciferase (pGL4.32[luc2P/NF-κB-RE/Hygro] vector (Promega, Southampton, UK, Cat#E8491) or NF-κB-luciferase (P. Baeuerle, Freiburg, Germany) and phRL-TK Renilla-luciferase expressing construct under constitutive thymidine-kinase promoter control (Promega, Cat#E6241) at a ratio of 14:1 for normalization in Dual-Luciferase assays (Promega) that were conducted using manufacturer's recommendations.

4.3 Molecular cloning of death-domain deficient ankyrin-G vectors (pAnkG-ΔDD) and the death-domain of ankyrin-G (DD of ankyrin-eGFP). For the generation of death-domain excised ankyrin-G vectors, we first digested 270kDa eGFP-N1-ankyrin-G using *ApaI* and column purified the linearized vector. Following double-digestion using *EcoRV* and *XbaI*, and subsequent to alkaline phosphatase (Fermentas) treatment, we re-ligated the long fragment back with the eGFP comprising C-terminal fragment following gel purification. We used the following primers to amplify the death domain of ankyrin-G from rat total DNA preparations: 5'ATGCAAGCTTGCCACCATGGTCCACATCGAAAAAGGTCCAC-3' and 5'-ATGCGGATCCATGGTGCCTGAAATATTCCCATAATC-3' which where inserted into EGFP-N1 following *HindIII* and *BamHI* digestion.

4.4 Animal Procedures. Animal procedures were carried out under a license from the Department of Health and Children of Ireland (B100/3688) and the Health

Products Regulatory authority (HPRA, AE19127/P005), were compliant with EC Directive 86/609/EEC for animal experiments and were previously approved by the Research Ethics Committee of the Royal College of Surgeons in Ireland (REC131 & 817).

4.5 Immunofluorescence and flow cytometry analyses. Fixation of live neurons was performed immediately following media removal. Notably, prolonged (>1 min) pre-fixation incubation in ice-cold PBS resulted in notably diminished immunoreactivity using phosphorylation-specific antibodies. Glass-sealed formaldehyde solutions (Mallinkrodt, Dublin, Ireland) were freshly diluted from 16% to 3% content using 1 x cytoskeletal buffer (CB buffer: 10 mM PIPES (pH 6.8), 150 mM NaCl, 5 mM EGTA, 5 mM β-D-glucose, 5 mM $MgCl_2$) and brought to 37 ºC before addition to the wells. Where applicable, extraction of live cells was performed at 4 ºC for 5 minutes in 1% (m/V) Triton-X-100 in 10 mM Na_3PO_4-buffer (pH 7.4), 1 mM $MgCl_2$, 3 mM $CaCl_2$, 150 mM NaCl. Solutions were pre-chilled before washes with cold PBS, and fixation. Cells were permeabilized following washes, using ice-cold HBSS containing 0.1% (w/v) Triton X-100, blocked for 30 minutes with 0.3% (w/v) Triton X-100 and 5% (v/v) HS in HBSS. They were incubated for 2 hours at room temperature or overnight at 4 ºC in primary antibody dissolved in 0.3% (w/v) Triton X-100, 1% (v/v) HS in HBSS. For the labeling of brain slices, mice were sacrificed with an overdose of pentobarbital and transcardially perfused with 2% (for the cortical slices) or 4% (for the cerebellar slices) paraformaldehyde in 0.1 M phosphate-buffered saline. Coronal vibratome slices were obtained (50 μm) and stained free-floating following blocking procedures. Brains from mice with a targeted deletion of the cerebellar form of ankyrin-G (Zhou et al., 1998) and their controls were stained following post-fixation overnight at 4 ºC. For immunofluorescence

analyses, we used the following antibodies: A mouse monoclonal anti-ankyrin-G (1:500, 463, Santa Cruz Biotechnology (scbt) Cat# sc-12719, RRID:AB_626674, Heidelberg, Germany), a rabbit polyclonal anti-(pan)-IKKα/β, (1:1000, H-470, scbt, Cat# sc-7607, RRID:AB_675667), a rabbit polyclonal anti-Ser177/Ser181-phosphorylated IKKα/β (pIKKα/β, 1:500, clone 16A6, Cell Signaling Technology (CST) Cat# 2697P, RRID:AB_10120863, Hitchin, UK), a rabbit polyclonal anti-Ser181-phosphorylated IKKα/β (pSer181-IKKα/β, 1:500, scbt, Cat# sc-23470, RRID:AB_331624), a goat polyclonal anti-Ser177/Ser181-phosphorylated IKKα/β (1:500, scbt, Cat# sc-23470-R, RRID:AB_2122159), a rabbit polyclonal anti-Thr183/Tyr185-phosphorylated SAPK/JNK antibody (1:500, CST, Cat# 9251, RRID:AB_331659), a rabbit polyclonal anti-Thr180/Tyr182-phosphorylated p38-MAPK antibody (1:500, CST, Cat# 9211, RRID:AB_331641), a rabbit polyclonal and a mouse monclonal anti-Ser536-phosphorylated p65 antibody (1:500, 93H1, CST, Cat# 4025S, RRID:AB_10827881 & 7F1, CST, Cat# 3036S, RRID:AB_331281), a mouse monoclonal phospho-S32/36-IκBα antibody (1:500, CST, Cat# 9246L, RRID:AB_2267145), and anti-calbindin (Swant, Bellinzona, Switzerland). Following three washes in ice-cold HBSS, cultures were incubated for 1 hour at RT with secondary antibodies raised against the appropriate species bearing tags with either Alexa–Fluor-488 or -568 (Gibco-Invitrogen). Photomicrographs were obtained using a SPOT RT SE 6 Camera (Diagnostic Instruments, Sterling Heights, USA) or an Eclipse TE 300 inverted microscope (Nikon, Kinston upon Thames, UK) with Mercury-arc light bulbs. A Zeiss 510 or 710 LSM (Carl Zeiss, Jena, Germany) was used for confocal image analyses. Co-localization analyses were performed using CoLocalizer Express® software (CoLocalizer research software, Japan&Switzerland) and ImageJ (NIH, Bethesda, MD, USA) using the 'colocalisation test' plug-in with

Costes approximation. Correlation of anti-phorphorylated IKK immunoreactivity with that against ankyrin-G was conducted in Matlab (Mathworks, Galway, Ireland). For Fluorescence-activated cell sorting (FACS) analysis on a BD-LSRII (BD Medical, Dun Laoghaire, Ireland), PC12 cells were transfected using Lipofectamine 2000. Two days following transfection, pre-warmed 2% formaldehyde in CB-buffer was applied for fixation. The reaction was quenched using 100 mM glycine in PBS (50%) and HBSS (50%), then spun at 2000 rpm for 5 minutes. Labelling was performed overnight with anti-pIKKα/β (1:500, CST) and anti-GFP (1:1000, B2, scbt, Cat# sc-9996, RRID:AB_627695) and anti-ankyrin-G (1:1000, scbt) and respective secondary antibody labelling. Experiments were run using two laser intensity settings. For detection, the following settings were used, FSC:450, SSC:270: eGFP (excitation 488/emission 525±25), Alexa-568 (561/605±20).

4.6 Proximity-ligation assays. Proximity-ligation assays were conducted on formaldehyde-fixed primary cortical neurons. Briefly, following standard immunofluorescence procedures including primary antibody incubation (rabbit anti-phospho-IKKα/β (1:500, CST), mouse anti-IKKβ (1:500, Abcam, Cat# ab52775, RRID:AB_881558) or rabbit anti-IKKα/β (1:500, CST), and or with mouse monoclonal anti-ankyrin-G (1:500, scbt, were used overnight), incubation of Olink-specific plus/minus oligonucleotide-linked antibodies in antibody-dilution buffer followed (Duolink, Olink Bioscience, Uppsala, Sweden). Hybridisation of oligonucleotides and detection was conducted as advised in the manufacturer's instructions, washes were performed with HBSS solutions.

4.7 Western-blot. For Western-blot analyses cells were lysed in RIPA buffer (150 mM NaCl, 1.0% IGEPAL CA-630, 0.5% sodium-deoxycholate, 0.1% sodium dodecyl sulphate, 50 mM Tris-HCl, pH 8.0, including protease and phosphatase

inhibitor cocktail). Following standard procedures for cell lysis and protein determination, equal amounts of proteins were separated by 8-15% gel electrophoresis as appropriate and blotted using semi-dry transfer (Biorad, Hercules, CA, USA). Following blocking procedures in 3-5% milk-TBS and 0.05% Tween-20, phosphorylation-specific antibodies were dissolved in Tris-buffered saline, 0.05% Tween-20, while 3% milk was included for pan-specific antibodies. The following antibodies were used in Western blotting, mouse monoclonal anti-ankyrin-G (1:1000, scbt), rabbit polyclonal anti-phospho-S536-p65 (1:500, CST), anti-pan-p65 (1:5000, F-6X, scbt, Cat# sc-8008, RRID:AB_628017), rabbit anti-IKKα/β (1:1000, H-470, scbt), rabbit polyclonal anti-pIKKα/β (1:500, CST), a rabbit polyclonal anti-pIκBα (1:500, CST, Cat# 5209S, RRID:AB_10829358), mouse monoclonal anti-α-Tubulin (dm1a, 1:5000, Sigma-Aldrich, Cat# T9026, RRID:AB_477593) and mouse monoclonal anti-GAPDH (1:1000, 6C5, Abcam, Cat# ab92412, RRID:AB_2278693). Detection was performed by incubation with the appropriate HRP-linked secondary antibody (Jackson Immunoresearch, Newmarket, UK).

4.8 Statistical analysis. We employed GraphPad Prism for statistical analyses (GraphPad Software Inc., La Jolla, USA). Parametric testing was performed and we conducted staticstical analyses as detailed in the figure legends. All data are represented as mean ± S.E.M., unless stated otherwise. p values ≤ 0.05 were considered to be significantly different and marked by an asterisk.

Acknowledgments: The authors would like to thank Christian Schultz, Mannheim, Germany for tissue derived from cerebellar-specific ankyrin-G knock-out mice, originally generated in the group of Vann Bennett (Duke University Medical Center, Durham, NC, USA), whom we also thank for the kind provision of the 270 kDa ankyrinG-eGFP construct. Further, the authors would like to thank Ina Woods for technical assistance; Jasmin Schmid for generation of the correlation plot in MatLab; Dr. Heiko Düssmann for his help with confocal microscopy and Dr. Christian Hellwig for his assistance with the fluorescence-assisted cell sorter.

Funding:

This work was supported by Science Foundation Ireland [08/IN.1/B1949; 14/IA/2582] and the European Union [EU FP7-EpiMiRNA under agreement Nr. 602130]. The authors declare that they have no conflict of interest.

References.

Baranauskas, G., David, Y., Fleidervish, I.A., 2013. Spatial mismatch between the Na+ flux and spike initiation in axon initial segment. Proc Natl Acad Sci U S A. 110, 4051-6.

Beg, A.A., et al., 1995. Constitutive NF-kappa B activation, enhanced granulopoiesis, and neonatal lethality in I kappa B alpha-deficient mice. Genes Dev. 9, 2736-46.

Bender, K.J., Trussell, L.O., 2009. Axon initial segment Ca2+ channels influence action potential generation and timing. Neuron. 61, 259-71.

Brachet, A., et al., 2010. Ankyrin G restricts ion channel diffusion at the axonal initial segment before the establishment of the diffusion barrier. J Cell Biol. 191, 383-95.

Buffington, S.A., et al., 2012. IkappaBalpha is not required for axon initial segment assembly. Mol Cell Neurosci. 50, 1-9.

Bui, N.T., et al., 2001. Activation of nuclear factor kappaB and Bcl-x survival gene expression by nerve growth factor requires tyrosine phosphorylation of IkappaBalpha. J Cell Biol. 152, 753-64.

Burke, J.R., et al., 2003. BMS-345541 is a highly selective inhibitor of I kappa B kinase that binds at an allosteric site of the enzyme and blocks NF-kappa B-dependent transcription in mice. J Biol Chem. 278, 1450-6.

Cavalli, V., et al., 2005. Sunday Driver links axonal transport to damage signaling. J Cell Biol. 168, 775-87.

Chen, Z., et al., 1995. Signal-induced site-specific phosphorylation targets I kappa B alpha to the ubiquitin-proteasome pathway. Genes Dev. 9, 1586-97.

Del Rio, M., et al., 2004. The death domain of kidney ankyrin interacts with Fas and promotes Fas-mediated cell death in renal epithelia. J Am Soc Nephrol. 15, 41-51.

Emmanouil, M., et al., 2009. Neuronal I kappa B kinase beta protects mice from autoimmune encephalomyelitis by mediating neuroprotective and immunosuppressive effects in the central nervous system. J Immunol. 183, 7877-89.

Feldman, M., Cryer, B., 1999. Aspirin absorption rates and platelet inhibition times with 325-mg buffered aspirin tablets (chewed or swallowed intact) and with buffered aspirin solution. Am J Cardiol. 84, 404-9.

Freal, A., et al., 2016. Cooperative Interactions between 480 kDa Ankyrin-G and EB Proteins Assemble the Axon Initial Segment. J Neurosci. 36, 4421-33.

Gasser, A., et al., 2012. An ankyrinG-binding motif is necessary and sufficient for targeting Nav1.6 sodium channels to axon initial segments and nodes of Ranvier. J Neurosci. 32, 7232-43.

Gaudreault, P., Temple, A.R., Lovejoy, F.H., Jr., 1982. The relative severity of acute versus chronic salicylate poisoning in children: a clinical comparison. Pediatrics. 70, 566-9.

Gerdts, J., et al., 2011. Image-based screening identifies novel roles for IkappaB kinase and glycogen synthase kinase 3 in axonal degeneration. J Biol Chem. 286, 28011-8.

Goetze, B., et al., 2003. Coupling the iron-responsive element to GFP--an inducible system to study translation in a single living cell. Sci STKE. 2003, PL12.

Grilli, M., et al., 1996. Neuroprotection by aspirin and sodium salicylate through blockade of NF-kappaB activation. Science. 274, 1383-5.

Kaltschmidt, C., et al., 1994. Constitutive NF-kappa B activity in neurons. Mol Cell Biol. 14, 3981-92.

Kole, M.H., et al., 2008. Action potential generation requires a high sodium channel density in the axon initial segment. Nat Neurosci. 11, 178-86.

Konig, H.G., et al., 2012. Fibroblast growth factor homologous factor 1 interacts with NEMO to regulate NF-kappaB signaling in neurons. J Cell Sci. 125, 6058-70.

Konig, H.G., et al., 2017. NF-kappaB regulates neuronal ankyrin-G via a negative feedback loop. Sci Rep. 7, 42006.

Kretschmer, T., et al., 2004. Elevated ankyrin G in a plexiform neurofibroma and neuromas associated with pain. J Clin Neurosci. 11, 886-9.

Lavrik, I., Golks, A., Krammer, P.H., 2005. Death receptor signaling. J Cell Sci. 118, 265-7.

Lou, J.Y., et al., 2005. Fibroblast growth factor 14 is an intracellular modulator of voltage-gated sodium channels. J Physiol. 569, 179-93.

Meffert, M.K., et al., 2003. NF-kappa B functions in synaptic signaling and behavior. Nat Neurosci. 6, 1072-8.

Mercurio, F., et al., 1997. IKK-1 and IKK-2: cytokine-activated IkappaB kinases essential for NF-kappaB activation. Science. 278, 860-6.

Politi, C., et al., 2008. Accumulation of phosphorylated I kappaB alpha and activated IKK in nodes of Ranvier. Neuropathol Appl Neurobiol. 34, 357-65.

Pradere, J.P., et al., 2016. Negative regulation of NF-kappaB p65 activity by serine 536 phosphorylation. Sci Signal. 9, ra85.

Rasmussen, H.B., et al., 2007. Requirement of subunit co-assembly and ankyrin-G for M-channel localization at the axon initial segment. J Cell Sci. 120, 953-63.

Sakurai, H., et al., 2003. Tumor necrosis factor-alpha-induced IKK phosphorylation of NF-kappaB p65 on serine 536 is mediated through the TRAF2, TRAF5, and TAK1 signaling pathway. J Biol Chem. 278, 36916-23.

Sanchez-Ponce, D., et al., 2008. New role of IKK alpha/beta phosphorylated I kappa B alpha in axon outgrowth and axon initial segment development. Mol Cell Neurosci. 37, 832-44.

Schmeisser, M.J., et al., 2012. IkappaB kinase/nuclear factor kappaB-dependent insulin-like growth factor 2 (Igf2) expression regulates synapse formation and spine maturation via Igf2 receptor signaling. J Neurosci. 32, 5688-703.

Schultz, C., et al., 2006. Coincident enrichment of phosphorylated IkappaBalpha, activated IKK, and phosphorylated p65 in the axon initial segment of neurons. Mol Cell Neurosci. 33, 68-80.

Simpson, C.S., Morris, B.J., 2000. Regulation of neuronal cell adhesion molecule expression by NF-kappa B. J Biol Chem. 275, 16879-84.

Soderberg, O., et al., 2007. Proximity ligation: a specific and versatile tool for the proteomic era. Genet Eng (N Y). 28, 85-93.

Strickson, S., et al., 2013. The anti-inflammatory drug BAY 11-7082 suppresses the MyD88-dependent signalling network by targeting the ubiquitin system. Biochem J. 451, 427-37.

Tarantino, N., et al., 2014. TNF and IL-1 exhibit distinct ubiquitin requirements for inducing NEMO-IKK supramolecular structures. J Cell Biol. 204, 231-45.

Wang, C., et al., 2001. TAK1 is a ubiquitin-dependent kinase of MKK and IKK. Nature. 412, 346-51.

Wildburger, N.C., et al., 2015. Quantitative proteomics reveals protein-protein interactions with fibroblast growth factor 12 as a component of the voltage-gated sodium channel 1.2 (nav1.2) macromolecular complex in Mammalian brain. Mol Cell Proteomics. 14, 1288-300.

Yang, J., et al., 2015. Pathological axonal death through a MAPK cascade that triggers a local energy deficit. Cell. 160, 161-76.

Yin, M.J., Yamamoto, Y., Gaynor, R.B., 1998. The anti-inflammatory agents aspirin and salicylate inhibit the activity of I(kappa)B kinase-beta. Nature. 396, 77-80.

Yu, P., et al., 2013. Global analysis of neuronal phosphoproteome regulation by chondroitin sulfate proteoglycans. PLoS One. 8, e59285.

Zandi, E., et al., 1997. The IkappaB kinase complex (IKK) contains two kinase subunits, IKKalpha and IKKbeta, necessary for IkappaB phosphorylation and NF-kappaB activation. Cell. 91, 243-52.

Zandi, E., Chen, Y., Karin, M., 1998. Direct phosphorylation of IkappaB by IKKalpha and IKKbeta: discrimination between free and NF-kappaB-bound substrate. Science. 281, 1360-3.

Zhang, X., Bennett, V., 1998. Restriction of 480/270-kD ankyrin G to axon proximal segments requires multiple ankyrin G-specific domains. J Cell Biol. 142, 1571-81.

Zhou, D., et al., 1998. AnkyrinG is required for clustering of voltage-gated Na channels at axon initial segments and for normal action potential firing. J Cell Biol. 143, 1295-304.

Figure legends.

Figure 1: Phosphorylated Ser177/181- and Ser181-IKKα/β-directed antibodies decorate the AIS in molecular proximity to IKKα/β-specific antibodies. (**A,B**) Mature mouse cortical neurons were formaldehyde (3%) fixed at 37 °C for 12 minutes and first incubated with anti-phospho-Ser177/181-IKKα/β (red, A) or anti anti-phospho-Ser181-IKKα/β (red, B) and ankyrin-G (green) specific antibodies and then appropriate fluorescently tagged secondary antibodies. (**C**) Mature cortical neurons were fixed as above and exposed to anti-phospho-p38 MAPK-specific antibodies (red). A phospho-IκBα-directed antibody was used to highlight the AIS (5A5, green). (**D**) Mature cortical neurons were fixed as above and exposed to anti-phospho-JNK/SAPK specific antibodies (red), and co-labeled with anti-ankyrin-G (green). (**E,F**) Cytosolic proteins were extracted from cultured cortical neurons on DIV 18 using a triton-X-100 extraction protocol for 5 min on ice. Subsequent to rapid formaldehyde fixation, the cultures were immunolabeled with anti-phospho-Ser177/181-IKKα/β (red, E), or anti-phospho-SAPK/JNK (red, F), together with ankyrin-G specific antibodies (green). (**G-I**) Schematic cartoon and results of the proximity-ligation assay for verification of epitopes in close proximity. Fixed mature cortical neurons were exposed to rabbit and mouse-derived anti pan-IKKα/β together with anti-phospho-Ser177/181-IKKα/β specific antibodies, followed by appropriate secondary oligonucleotide-linked antibody incubation, hybridization and rolling circle amplification (red). Ankyrin-G-specific antibodies (green) were used to identify the AIS. Note the accumulation of PLA-dots in the ankyrin-G-specific area (arrows in H). For quantification, the proximal dendritic area was estimated by drawing a circle around the cell body with the radius of the AIS and the somatic area was estimated by

drawing a circle with a center in the nucleus with a radius equivalent to the distance to the beginning of the AIS (I, n=15-19 cells, Box and Whiskers plot ± Tukey range, Kruskal-Wallis test). Peptide sequences around phosphorylation sites are shown (A-D). Boxed areas highlight exemplary AIS'. Scale bars, 10 μm.

Figure 2: Small-hairpin-mediated RNA interference of IKKβ from mature neurons reduces anti-phosphorylated IKKα/β immunofluorescence intensity in the AIS. (**A,B**) Neuro-2A cells were transfected with an IKKβ expression plasmid (1st lane), four different IKKβ-specific ('A'-'D') or control shRNA constructs. The cells were cultured for four days, lysed in RIPA-buffer and subjected to Western-blot procedure. A representative Western-blot is depicted in (A), the optical density relative to loading control was determined from 2-4 silencing experiments in (B). (**C-D**) DIV6-9 primary cultured cortical neurons were transfected with either constructs 'A' or 'C' as used above, or their combination, and incubated for 4 days. Following formaldehyde fixation (3%) for 12 minutes, neurons were subjected to immunofluorescent labeling using anti-phospho-Ser177/181-IKKα/β (red). eGFP (green), co-expressed from the same plasmids is depicted for transfection control (C). Arrows highlight exemplary AIS'. Profile of pIKKα/β immunofluorescence intensities along the AIS (D; n = 225-239 cells per group).

Figure 3: Phosphorylated IKKα/β immunoreactivity colocalizes with ankyrin-G immunoreactivity in the AIS during development *in vitro* and *in vivo*. (**A-C**) Mouse cortical neurons were cultured for two weeks, fixed by paraformaldehyde (3%)

incubation for 12 minutes and immunolabeled using phospho-Ser177/181-IKKα/β (red) and ankyrin-G (green) specific antibodies and imaged using a confocal microscope (A&B). At higher magnification a dotted ~~pattern of~~ anti pIKKα/β immunoreactivity ~~becomes apparent~~ was detectable that co-localized with ankyrin-G immunoreactivity ~~to a high degree~~ (Pearson's correlation coefficient R=0.8305 from 3 planes of a stack of confocal images, B). Immunoreactivity intensities of phospho-Ser177/181-IKKα/β and ankyrin-G were measured from the end of the soma along the AIS and graphed against each other following normalization to their starting point in the AIS, the distance from the soma was color-coded using Matlab (C, n = 38 AIS', Spearman correlation coefficient of mean curve = 0.97). (**D**) Cortical neurons were fixed on DIV4, 7, 14 and 18, and co-immunolabeled with anti-pIKKα/β and ankyrin-G antibodies. (**E**) A mouse was perfused with 3% paraformaldehyde, the brain removed and brain slices obtained. Following pepsin-treatment (Konig et al., 2012), the free-floating slices were co-immunolabeled using phospho-Ser177/181-IKKα/β and ankyrin-G-specific antibodies. Scale bars, 10 μm.

Figure 4: Phosphorylated IKKα/β immunoreactivity is in molecular proximity with ankyrin-G immunoreactivity in the AIS. (**A-D**) The schematic cartoon highlights the principle of the proximity-ligation assay using anti-ankyrinG (raised in mouse) and anti-pIKKα/β-(raised in rabbit) specific antibodies (A). Mature cultured mouse cortical neurons were paraformaldehyde fixed, and incubated with ankyrin-G and pIKKα/β–specific antibodies and PLA assays performed (red). Ankyrin-G specific immunofluorescence was additionally obtained by incubation with anti-mouse-Alexa488 (green, B). The boxed area was obtained at higher magnification and

shown in (C). For quantification, the somatic and proximal dendritic area was estimated by drawing a circle around the cell body with the radius of the AIS, the number of PLA-spots in the ankyrin-G positive AIS versus somato-dendritic PLA spots was determined. Omission of primary antibody in the reaction served as negative control (D, n=23-29 axons, Box and Whiskers plot ± Tukey range, t-test). (**E**) Phosphorylated-IKKα/β does not accumulate in the proximal axon (arrows) of ankyrin-G-deficient Purkinje cells. Cerebellar slices from ankyrin-G-deficient or wild-type mice were stained using calbindin- (green; to mark Purkinje-cells) and phospho-IKKα/β-specific (red) antibodies. Scale bars, 10 μm.

Figure 5: Phosphorylated IKKα/β immunoreactivity co-localizes to pIκBα and p-p65 immunoreactivity in the AIS. Phosphorylated IKKα/β and p-p65 levels are increased by ankyrin-G overexpression. (**A**) Mouse cortical neurons were fixed and immunofluorescence using phosphorylated IKKα/β (rabbit, green) and Ser536-phosphorylated p65/NF-κB (pp65, mouse, red) antibodies was obtained. (**B**) Mouse cortical neurons were fixed and immunofluorescence using phosphorylated IKKα/β (rabbit, scbt, red) and anti-phosphorylated IκBα (5A5, CST, mouse, red) was obtained. Boxed area magnified below highlight membranous (arrows, red) and cytosolic immunoreactivities (green). (**C**) Rat PC12 cells were transfected with increasing amounts of ankyrin-G-eGFP and/or a constant amount of an IKKβ expression vector, and lysates subjected to Western-blotting procedure following 3 days of expression. (**D**) Twenty-four hours following transfection, flow cytometry was performed on fixed PC12 cells. Cells were transfected using eGFP or eGFP&IKKβ (black) and AnkG-eGFP (red) or AnkG-eGFP&IKKβ and stained with

anti-pIKKα/β. GFP-positive (GFP^+) cells were gated and the AUC of pIKKα/β immunofluorescence intensities were determined (from n = 2 cultures each including controls with comparable results, GFP-fluorescence positive cells were gated from n = 8,400-10,000 cells based on background fluorescence from non-transfected controls). (**E**) Cortical neurons were transfected with eGFP and/or IKKβ and/or ankG-eGFP. Following expression for two days the neurons were fixed and immunolabeled with Ser536-phosphorylated p65-specific antibodies. Arrows highlight prominent pp65-AIS immunoreactivity. Scale bars, 10 μm. (**F**) Schematic drawings of the Ankyrin-G constructs used below, M=membrane-binding domain, SP=Spectrin-binding domain, SR=Serine-rich domain, T=tail, DD=Death-domain (adapted from (Zhang and Bennett, 1998)). (**G**) PC12 cells were transfected with a small-hairpin RNA transcribing vector directed at ankyrin-G or a small-hairpin control vector together with a NF-κB response element (NF-κB-RE) reactive firefly luciferase reporter vector and a constitutive renilla-luciferase vector as transfection control. Mann-Whitney test, *p=0.0079, n=4 cultures from one plating. (**H**) PC12 cells were transfected with an eGFP vector or ankyrin-G eGFP together with the NF-κB-RE dual-luciferase vectors for one day. n=4 cultures from one plating. (**I**) PC12 cells were transfected with an eGFP vector, ankyrin-G-eGFP, ankyrin-G-eGFP deficient in the death-domain (ΔDD) together with the NF-κB dual-luciferase vectors, respectively. n=3 experiments. (**J**) PC12 cells were transfected with eGFP or a vector containing the death-domain of ankyrin-G linked to eGFP together with the NF-κB dual luciferase vectors. n=4 cultures from one plating. 1 value removed following ROUT outlier detection, n=4. (F-I) Dual-luciferase assays were conducted following cell lysis in passive lysis buffer on day one.

Figure 6. IKK-inhibitors deplete AIS-phospho-IKKα/β immunofluorescence. (**A,B**) Mature cortical neurons were incubated with distinct inhibitors of the IKK-complex or upstream signaling. BMS-345541, Bay11-7082, IKK-inhibitor VII or manumycin were added to the culture media at three different concentrations for 2 hours (n = 31-242 neurons pooled from 1-3 wells and 3-6 fields of view/treatment, Kruskal-Wallis test, Dunn's *post-hoc*, scale bars 10 µm). (**C**) Mature cortical neurons were incubated with two concentrations of acetylsalicylic acid (ASA) for twenty-four hours and the relative normalized immunofluorescence intensities of phosphorylated IKKα/β determined and plotted along the AIS. **(D)** Quantification of the single trace immunofluorescence intensities as determined in 'C' and depicted as AUC (6-17 axon traces, 'Box and Whiskers with Tukey range', Kruskal-Wallis test, Dunn's *post-hoc*, p=0.026).

A constitutively-active IKK-complex at the axon initial segment

Hans-Georg König[a,b,*], Orla Watters[a,b], Sinéad Kinsella[a,b,#], Mohammed Ameen[a], Beau J. Fenner[a,¶] and Jochen H. M. Prehn[a,b,*]

[a]Department of Physiology and Medical Physics, Royal College of Surgeons in Ireland, 123 Saint Stephen's Green, Dublin 2, Ireland); [b]Centre for the Study of Neurological Disorders, Royal College of Surgeons in Ireland, 123 Saint Stephen's Green, Dublin 2, Ireland; [#]Present address: Program in Immunology, Clinical Research Division, Fred Hutchinson Cancer Research Center, 1011 Fairview Avenue N.,Seattle, WA 98109, USA. [¶]Present address: Singapore National Eye Centre, 11 Third Hospital Avenue, Singapore 168751, Singapore.

Authors' e-mail: H.G.K: hgkoenig@rcsi.ie; O.W.: orlawatters@rcsi.ie; S.K.: sineadkinsella@rcsi.ie; M. A.: mohammedameen@rcsi.ie; B.F.: beaufenner@gmail.com; J.H.M.P.: prehn@rcsi.ie

***Corresponding authors:** HGK (hgkoenig@rcsi.ie) & JHMP (prehn@rcsi.ie); Tel.: + 353 1 402 2260; Fax.: +353 1 402 2447

Text pages: 31

Figures: 6

Number of words in the Abstract: 161

Number of words in the Introduction: 500

Number of words in the Results: 1361

Number of words in the Discussion: 987

Number of words in Experimental procedure: 1457

Number of words in Figure Legends: 1323

Abbreviations: AIS, axon initial segment; ASA, acetyl-salicylic acid; DMEM, Dulbecco's modified Eagle media; eGFP; enhanced green-fluorescent protein; FADD, Fas-associated death domain; FBS, fetal bovine serum; FGF, fibroblast growth factor; FSC, forward scatter; HBSS, Hanks' Balanced Salt solution; HS, horse serum; HRP, horseradish peroxidase; IGEPAL, Octylphenoxy poly(ethyleneoxy)ethanol, branched; IκBα, inhibitor of κB–α; IKK, IκB-kinase; IL-1, interleukin-1; JNK, c-Jun N-terminal kinases; KCNQ, delayed rectifier potassium channel, voltage-gated, KQT-like subfamily; MAPK, mitogen-activated protein kinase; MAPKK, mitogen-activated protein kinase kinase; NEMO, NF-κB essential modulator (IKKγ); NF-κB, Nuclear factor kappa-light-chain-enhancer of activated B cells; PC12 Phaeochromocytoma 12; PLA, proximity ligation assays; PIPES, 1,4-Piperazinediethanesulfonic acid; RPMI, Roswell Park Memorial Institute media; R-type calcium channel, resistant/residual opening calcium channels; Rel, retikuloendotheliosis; shRNA, small-hairpin RNA; SAPK, stress-activated protein kinases; SSC, sideward scatter; TNF-α, tumor necrosis factor-α; TRADD, tumor necrosis factor receptor type 1-associated death domain protein; T-type calcium channel, transient opening calcium channels

Abstract.

Background: Previous studies provided evidence for an accumulation of IκB-kinase (IKK) α/β at the axon initial segment (AIS), a neuronal compartment defined by ankyrin-G expression. Here we explored whether the presence of the IKK-complex at the AIS was associated with the activation of IKK signaling at this site. Methods and Results: Proximity-ligation assays (PLAs) using pan-IKKα/β, phospho-IKKα/β-specific as well as ankyrin-G specific antibodies validated their binding to proximal epitopes in the AIS, while antibodies to other phosphorylated signaling proteins showed no preference for the AIS. Small-hairpin mediated silencing of IKKβ significantly reduced anti-phospho-IKKα/β-immunoreactivities in the AIS. *ank3* gene-deficient cerebellar Purkinje cells also exhibited no phosphorylated IKKα/β at the proximal region of their axons. Transient ankyrin-G overexpression in PC12 cells augmented NF-κB transactivation in an ankyrin-G death-domain dependent manner. Finally, small molecule inhibitors of IKK-activity, including Aspirin, inhibited the accumulation of activated IKK proteins in the AIS. Conclusion: Our data suggest the existence of a constitutively-active IKK signaling complex in the AIS.

Keywords: axon initial segment; NF-κB; IKK 2 Kinase; ankyrin-G; proximity ligation assay; axon

1. Introduction.

In the central nervous system, the transcription factor nuclear factor-κB (NF-κB) is regularly composed of p50, p65/RelA and c-Rel-containing heterodimers. Inactive NF-κB is sequestered in the cytosol by association with its inhibitor of κB (IκBα) (Chen et al., 1995). Phosphorylation of IκBα by the inhibitor of κB-kinase (IKK)-complex results in the degradation of the protein and liberation of NF-κB for translocation into the nucleus (Zandi et al., 1998). IKKα/β occurs as heterodimers or homodimers and associates with IKKγ to compose the IKK signalosome. Autophosphorylation of IKKα/β within its activation domain, resulting in the phosphorylation of Ser177/181 of human IKKβ and Ser176/180 of human IKKα, have been suggested as essential in their activation mechanism (Mercurio et al., 1997) (Zandi et al., 1997). NF-κB is constitutively active in the CNS (Kaltschmidt et al., 1994) and inducible in response to neuronal activity (Meffert et al., 2003) as well as cytokine treatment (Bui et al., 2001). NF-κB drives the transcription of a wide range of target genes in neurons, such as pro-survival genes (Bui et al., 2001), neuronal adhesion molecules (Simpson and Morris, 2000), proteins regulating synaptogenesis and synaptic maturation (Schmeisser et al., 2012) and cytoskeletal anchor proteins including ankyrin-G (Konig et al., 2017).

Ankyrin-G is essential for the assembly and maintenance of the axon initial segment (AIS)(Freal et al., 2016), a neuronal compartment that in most neurons is required to convert synaptic input into action potential generation (Baranauskas et al., 2013; Kole et al., 2008). Ankyrin-G sequesters ion channels including the sodium channels $Na_V1.2$ (Brachet et al., 2010) and $Na_V1.6$ (Gasser et al., 2012), and the M-current potassium channels KCNQ2/3 (Rasmussen et al., 2007). Voltage-gated T and

R-type calcium-channels co-localize with sodium channels in the AIS and modulate spike frequency and timing (Bender and Trussell, 2009). Fibroblast-growth factor homologous factors, FGF12-14 are intracellular proteins that regulate sodium-channel activity at the AIS (Lou et al., 2005; Wildburger et al., 2015).

Others and we had previously described that immunoreactivity against the upstream kinase of NF-κB, IKKα/β, could be found at the AIS and at the nodes of Ranvier in neurons at rest (Politi et al., 2008; Sanchez-Ponce et al., 2008; Schultz et al., 2006). In subsequent studies, pan-p65, pan-IKKα/β (Konig et al., 2017) as well as pan-NEMO immunoreactivity (Konig et al., 2012; Konig et al., 2017) were also found at the AIS following detergent extraction, a method used to carefully remove proteins that are not associated with the cytoskeleton. However a single previous report also demonstrated that immunoreactivity against the phosphorylated IκBα protein at the AIS persisted in IκBα gene-deficient mice (Buffington et al., 2012), questioning the presence of NF-κB signaling components at the AIS.

Using proximity-ligation assays, small-hairpin mediated gene silencing, gene deficient mice and pharmacological approaches, we here set out to investigate whether phosphorylated components of the NF-κB cascade localize to the AIS, and whether IKK activity is required for the accumulation of active, phosphorylated p65 at the AIS. Our data suggest the presence of a constitutively-active IKK signaling complex in the AIS.

2. Results.

2.1 Multiple anti-phosphorylated IKKα/β-antibodies label the AIS and their epitopes can be found in molecular proximity to AIS-bound pan-IKKα/β antibodies.

We had previously shown that IKK, the upstream kinase of IκBα, is present in the AIS (Konig et al., 2012; Konig et al., 2017). Using mature mouse cortical neurons, we found that significant anti-phosphorylated IKKα/β (pIKK) immunoreactivity was detectable in the AIS, demarcated by anti-ankyrin-G immunoreactivity (Fig 1A-F). Anti-phosphorylated IKKα/β (pIKK) immunolabeling was reduced by prolonged washes with ice-cold phosphate-buffered saline solution (data not shown), and required immediate fixation using pre-warmed, buffered formaldehyde solutions, suggesting that carefully optimized conditions during fixation are required to detect the activated kinase. To test whether different antibodies raised against the phosphorylated IKKα/β epitope were reactive in the AIS, we used anti phospho-Ser177/181 IKKβ (Ser176/180-IKKα) antibodies, as well as antibodies raised against anti-phospho-Ser181 IKKβ (Ser180 IKKα) only. Both types of antibodies were reactive in the AIS (Figure 1A&B), whereas antibodies raised against anti-phospho-Thr180/Tyr182 of p38α/MAPK14 or anti-phospho-Thr183/Tyr185 SAPK/JNK did not show enhanced immunolabeling in the AIS (Figure 1C&D). The latter kinases have been shown to be involved in axonal stress response pathways (Cavalli et al., 2005; Gerdts et al., 2011; Yang et al., 2015). Anti-phosphorylated IKKα/β immunoreactivities in the AIS were preserved following extraction of cytosolic proteins, however anti-phosphorylated SAPK/JNK immunoreactivities showed no AIS staining following detergent extraction (Figure 1E&F). As a further test for antibody-specificity, we employed proximity-ligation assays (PLA) between pan-

specific and phospho-specific IKKα/β antibodies. PLA-dots appear where both antibodies bind within ca. 40 nm from each other (Soderberg et al., 2007)(Schematic Figure 1G). Significantly more PLA-products were detected along the ankyrin-G-positive AIS and in the soma of neurons than in a comparable dendritic area (Figure 1H&I). These data suggested that anti-pan and anti-phosphorylated IKKα/β immunoreactivity bind to the same protein in the AIS.

2.2 IKKβ-silencing reduces anti-phosphorylated IKKα/β immunofluorescence intensities in the AIS.

We previously showed IKKβ protein presence at the AIS (Konig et al., 2017). To further substantiate our findings and to demonstrate antibody specificity, we employed small-hairpin constructs directed at IKKβ mRNA. To test the efficiency of four different small-hairpin vector constructs, we transfected murine Neuro-2A cells for four days with the relevant constructs. We also included cells transfected with an IKKβ expression plasmid as a positive control. IKKβ protein abundance was effectively diminished by IKKβ shRNA sequences 'A' and 'C' (Figure 2A,B). We then performed small-hairpin RNA-mediated silencing of IKKβ for 4 days in mature cortical neurons with eGFP (enhanced green fluorescent protein) expressed from the same plasmid. Following immunolabeling using anti-phosphorylated IKKα/β antibodies, we detected a decreased immunoreactivity along the AIS in cells transfected with IKKβ 'A' and 'C' small-hairpin constructs (Figure 2C,D). The mean (and median) area under the curve of pIKKα/β immunofluorescence along the AIS was strongly decreased by co-transfection of IKKβ 'A' and 'C' shRNAs from 65.80 ± 2.93 by 12.37 ± 3.22 (n = 225-239 cells per group, p=0.0003; by 9.72 ± 3.64 for 'C').

The decreased cellular IKKβ protein abundance thus reduced IKKβ levels at the AIS and hence immunofluorescence intensity using phosphorylation-specific antibodies.

2.3 Phosphorylated IKK co-localizes and interacts with ankyrin-G in vitro and in vivo.

We next investigated whether ankyrin-G and phosphorylated Ser176/177&180/181-IKKα/β immunoreactivities co-localized along the proximal axon of neurons. We stained mature cortical neurons with anti-phosphorylated IKKα/β and ankyrin-G specific antibodies, and plotted the normalized immunofluorescence intensities of ankyrin-G and phosphorylated IKKα/β along the AIS against each other. Co-localization of the highest pixel intensities for the pIKKα/β and ankyrin-G staining was found in a punctate pattern along the AIS suggesting the proteins co-localized in vesicular compartments along the AIS (Figure 3A&B). Anti-phosphorylated IKKα/β and anti-ankyrin-G immunoreactivity intensities correlated along the ankyrin-G positive AIS stretch, only minimally deviating from an ideal correlation (dotted line) of pixel intensities (Figure 3C). Next, we examined whether expression levels and localization during axonal development *in vitro* concurred to provide evidence in support of a co-developmental pattern. We found that phosphorylated IKKα/β and ankyrin-G immunoreactivities increased in parallel at the AIS during development from DIV4 to DIV18 (Figure 3D). Of note, we observed the co-clustering of ankyrin-G and phospho-IKKα/β immunoreactivities in brain slices derived from the cerebral cortex following immediate and mild brain fixation *in vivo* (Figure 3E). To further analyze whether anti-phospho-IKKα/β were found in molecular proximity (≲40 nm) to ankyrin-G epitopes, we employed proximity-ligation assays (PLA, Schematic Figure 4A). We found that PLA spots

densely clustered along proximal axons, indicating molecular proximity between phosphorylated-IKKα/β and ankyrin-G *in situ*, and they occurred in significantly higher numbers along the AIS than within the somatic compartment (Figure 4B-D). We next examined whether *ank3*/ankyrin-G gene knockout ablated IKK-phosphorylation in the AIS. Mice with a cerebellar-specific knockout of ankyrin-G were deficient in phosphorylated IKKα/β at the proximal region of cerebellar Purkinje cell axons (Figure 4E).

2.4 Ankyrin-G overexpression increases IKK-phosphorylation levels and NF-κB activity in a death-domain dependent fashion in cells devoid of an AIS.

In further immunolabeling studies, we found AIS immunoreactivity for two downstream targets of IKKα/β kinase activity in the AIS [see also (Pradere et al., 2016; Sakurai et al., 2003; Zandi et al., 1998)]. Immunoreactivity against phosphorylated p65 and phosphorylated IκBα could be detected in the AIS using mouse monoclonal antibodies (clone 7F1) directed at Ser536 of p65 (Ser534 in mouse p65) and (clone 5A5) directed at Ser32/36-phosphorylated IκBα (Figure 5A&B), further suggesting the existence of a constitutively-active IKK-complex at the AIS. We took two different experimental approaches to test this hypothesis. In a first approach, we performed experiments in neuronal-like phaeochromocytoma-cell line 12 (PC12) cells that are devoid of an AIS. Here, we explored whether ectopic Ankyrin-G expression was sufficient to activate IKK signaling. Ankyrin-G isoforms of 190, 270 and 480 kDa length are found at the AIS. The 480 kDa variant, bearing a long, neuron-specific tail-domain is indispensable for the accumulation of the two other isoforms of this scaffolding protein at this site (Freal et al., 2016). We tested whether increased IKK-phosphorylation could be induced by ectopic ankyrin-G

expression of the 270 kDa isoform in PC12 cells. Cells were transfected with increasing levels of ankyrin-G expression vectors together with or without plasmids encoding IKKβ. We found that higher ankyrin-G levels coincided with higher levels of phosphorylated IKKα/β. This was accompanied by increased levels of phospho-Ser32,36-IκBα and phospho-Ser536-p65, both downstream targets of the IKK-kinase (Figure 5C). In flow cytometry analyses we furthermore assessed how anti-phospho IKKα/β immunoreactivity was affected by co-transfection of both plasmids. More PC12 cells had high anti-phospho-IKKα/β immunoreactivity following ankyrin-G-eGFP and IKKβ-plasmid co-expression compared to cells expressing ankyrin-G-eGFP constructs only (Figure 5D). Similarly, when co-expressed in mature cortical neurons, we found that overexpression of both plasmids resulted in an increased immunoreactivity against Ser536-p65 in the AIS compared to IKKβ-only or control-transfected cells (Figure 5E). We then silenced ankyrin-G transiently for one day in PC12 cells and noticed a significant reduction of NF-κB transactivation potential (Figure 5G). Transiently overexpressing ankyrin-G in PC12 cells for one day increased NF-κB activity (Figure 5F,H,I). This rise was partly dependent on the death-domain of 270 kDa ankyrin-G, as we observed reduced activity following transfection of a death-domain deficient ankyrin-G plasmid (Figure 5F,I). We then built a vector expressing the sequence of the isolated death-domain of ankyrin-G. Following overexpression in PC12 cells for one day, cells with the highest amount of transfected plasmid showed numerically increased NF-κB reporter gene activity (Figure 5J).

2.5 Aspirin and other IKK-inhibitors effectively decrease phosphorylated IKK accumulation at the AIS.

In a second approach, we tested whether IKK phosphorylation levels were attenuated by IKK inhibitors, including BMS-3435541, an allosteric inhibitor of IKKβ and α (Burke et al., 2003), IKK-inhibitor VII, an ATP-competitive inhibitor of the IKKs, Bay11-7082, a MyD88-dependent inhibitor of IKK activation (Strickson et al., 2013) and manumycin, a farnesyltransferase inhibitor that also affects IKK-phosphorylation. Addition of each of the four inhibitors to mature cultured cortical neurons dose-dependently decreased anti-phosphorylated-IKKα/β immunofluorescence intensities at the AIS within hours (Figure 6A&B). Additionally, we used acetylsalicylic acid (ASA, Aspirin®), an inhibitor of IKKβ at physiological concentrations *in vitro* and *in vivo* (Grilli et al., 1996; Yin et al., 1998). ASA significantly decreased phospho-IKKα/β immunofluorescence along the AIS in a dose-dependent manner (Figure 6C-D).

3. Discussion.

We here characterized the accumulation of activation-loop phosphorylated IKKβ and pharmacological ablation of its constitutive phosphorylation in the AIS in primary neurons. We found that antibodies to IKK and ankyrin-G bound in close proximity to phosphorylated IKK within the AIS and determined that small-hairpin mediated silencing and IKK inhibitors induced a significant reduction of phosphorylated IKKα/β immunoreactivity in the AIS.

In the present study, we demonstrate that activated IKK is constitutively expressed in the AIS of mouse cortical neurons. We demonstrate that gene-silencing of IKKβ following transient transfection of primary neurons resulted in a significant decrease in anti-phosphorylated IKKα/β immunoreactivity in the AIS. The mild, transient gene silencing strategy over four days in matured neurons ensured that the AIS could develop normally, but that IKKβ phosphorylation levels were diminished in the differentiated AIS. Previous studies demonstrated pan-IKKα/β and pan-NEMO immunoreactivity localized to the AIS (Konig et al., 2012; Konig et al., 2017), and their immunostaining was found in clusters reminiscent of those previously found during IL-1 and TNF-α stimulation (Tarantino et al., 2014). Thus all three members of the IKK-signalosome are present at the AIS. Immunoreactivity against phosphorylated IκBα in the AIS, the subject of an earlier controversy, was previously demonstrated in neurons (Sanchez-Ponce et al., 2008; Schultz et al., 2006). Control experiments included enhanced anti-phosphorylated IκBα immunoreactivity using IκBα phospho-mimetic mutants, and abolished phosphorylated IκBα immunoreactivity after pre-treatment of the tissue with alkaline phosphatase (Schultz et al., 2006). Immunoreactivity against phosphorylated IκBα in the AIS was,

however, preserved in a mouse model with a targeted deletion of the full IκBα (*nfkbia*$^{-/-}$) locus (Beg et al., 1995; Buffington et al., 2012). The authors of the latter study suggested that anti-phosphorylated IκBα antibodies decorate an unrelated phosphoprotein in the AIS, as phosphorylation-specific antibodies can be promiscuous and the AIS may contain high amounts of phospho-proteins. Indeed, a previous proteomic study identified roughly 2000 phosphopeptides in neurons (Yu et al., 2013). To address the proposed promiscuous nature of the AIS in terms of phospho-proteins, we also demonstrated that neither phospho-p38, nor phospho-JNK immunoreactivity were enriched in the AIS. Similar to the IKK-complex, both of these kinases can be activated by MAPKK activity that is induced by stress-stimuli, and share common upstream regulatory kinases, including TAK with IKK (Wang et al., 2001). Of note, we also detected the downstream target of the IκB-kinase, Serine536-phosphorylated p65 in the AIS. Our study also demonstrated that pan-IKKα/β and phosphorylated IKK were in direct molecular proximity. Hence while the current study cannot fully resolve the controversy regarding the presence of phosphorylated IκBα immunoreactivity at the AIS, our data and data from other groups clearly demonstrate the presence of a phosphorylated IKK-complex and other key NF-κB signal transduction pathway proteins (IKKγ/NEMO, p65) at this site. We also observed that phosphorylated IKKα/β and ankyrin-G co-localized during *in vitro* development, and were in molecular proximity to each other in the soma and the initial segment. Previous studies not only found that IKK activity was essential for axon formation (Emmanouil et al., 2009; Sanchez-Ponce et al., 2008), but also that genetic silencing of IKKβ was sufficient to delay axon degeneration (Gerdts et al., 2011). Collectively, these findings suggest that IKKα/β and ankyrin-G interactions are essential for axon physiology and pathology.

Increased expression levels of ankyrin-G and IKKβ resulted in increased phosphorylation of the IKK-complex and its downstream targets p65 and IκBα. Notably, ankyrin-G isoforms expressed at the AIS contain a death-domain (DD) in their C-terminal tail (Del Rio et al., 2004; Zhang and Bennett, 1998), which may facilitate recruitment of adapter molecules such as tumor necrosis factor receptor type 1-associated death domain protein (TRADD) or Fas-associated death domain (FADD) (Lavrik et al., 2005), thus enabling activation of ubiquitin ligases and downstream IKK-complex activation. Indeed we found that transient, short-term overexpression of ankyrin-G moderately increased NF-κB activity in PC12 cells in a manner that depended on the expression of the death-domain of ankyrin-G. Our findings hence suggest that the C-terminal death domain of ankyrin-G is implicated in the phosphorylation of the IKK-complex. We previously also found that the p65/NF-κB transcription factor controls constitutive ankyrin-G expression levels in primary neurons (Konig et al., 2017). While short-term expression of ankyrin-G in PC12 cells augmented NF-κB activity, we had previously observed that longer expression in primary neurons diminished the transactivating potential of NF-κB, demonstrating that the transcription factor controls ankyrin-G expression in a negative feedback-loop in neurons (Konig et al., 2017). Our earlier study and the findings from the current study propose the concept that constitutive NF-κB activity during *in vitro* development is first induced and then restrained by ankyrin-G expression, possibly in a succession of positive and negative feedback loops, because an intricate balance of IKK-activity is required for physiological axon and initial segment formation.

We also found that pharmacological inhibition of IKK resulted in decreased IKK-phosphorylation levels at the AIS. Importantly, these results suggest that the NF-κB pathway in the AIS may represent a target for pharmacological intervention. It may be

possible to reinstate physiological ankyrin-G expression levels by modulating IKK-complex activity at the AIS. For example, painful neuromas are associated with increased ankyrin-G and sodium-channel expression levels (Kretschmer et al., 2004). Acetylsalicylic acid inhibits IKKα/β (Grilli et al., 1996; Yin et al., 1998), and this inhibition occurs in a dose-range consistent with serum levels observed after administration of therapeutic, analgesic doses (Feldman and Cryer, 1999). Interestingly, salicylates also show pronounced CNS toxicity following chronic administration to children (Gaudreault et al., 1982) which could be linked to effects on ankyrin-G expression.

In summary, our data demonstrate the presence of an activated, phosphorylated IKK-kinase in the AIS of neurons, and demonstrate that IKK activation leads to the accumulation of downstream NF-κB signaling molecules at the AIS. We also demonstrate that the popular non-steroidal anti-inflammatory drug acetylsalicylic acid (Aspirin®) reduces IKK-phosphorylation in the AIS, an effect that may contribute to its peripheral analgesic and potentially neurotoxic effects.

4. Experimental Procedure

4.1 Chemicals and Reagents. Chemicals were purchased from Sigma-Aldrich (Wicklow, Ireland) unless stated otherwise. Aspirin (ASA) was purchased from Sigma and Bayer (Leverkusen, Germany). Cell culture media and supplements were obtained from Gibco-Invitrogen (Dun Laoghaire, Ireland).

4.2 Cell culture and dual-luciferase assays. Neuro-2A cells were cultured in 50% RPMI, 50% Opti-MEM, and including 5% Fetal Bovine Serum (FBS), 2 mM L-Glutamine and 1% Penicillin/Streptomycin. Phaeochromocytoma (PC) 12 cells were cultured in RPMI media supplemented with 10% Horse Serum (HS), 5% FBS, 2 mM L-Glutamine and 1% Penicillin Streptomycin. Cells were kept in tissue culture incubators with a humidified atmosphere of 37 ºC and 5% CO_2. Cells were passaged every 3-4 days. PC12 and Neuro-2A cells were transfected using Lipofectamine 2000 (Gibco-Invitrogen) and Roche HP reagent (Sigma) using standard manufacturer protocols. Following hysterectomy, E16 *C57BL/6* mouse embryos were obtained and their cerebral cortices separated from meninges, minced, homogenized and trypsin-digested for 20-30 min at 37 ºC. The cortical cell suspension was plated at ca. 300,000 cells per cm^2 in DMEM, 10% FBS, 2 mM Glutamine and 1% Penicillin/Streptomycin for one day. Subsequently the neurons were grown in Neurobasal (Gibco), 2% B27, 1% GlutaMAX (Gibco), or NMEM-B27 media (1xMEM, 1 mM sodium pyruvate, 26 mM $NaHCO_3$, 2 mM GlutaMAX, 2% B27 and 33 mM β-D-Glucose), including β-D-arabino-furanoside (0.6 μM, days-in-vitro (DIV) 1-3). Transfection of primary neurons was conducted using calcium precipitation as previously described at ambient CO_2 levels for 2-4 hours (Goetze et al., 2003). Enhanced transfection rates were achieved by plate centrifugation at 1,500 rpm followed by incubation for 30 minutes prior to dissolving the complexes in HBSS, 33 mM β-D-glucose, 1 mM pyruvate and

15 mM HEPES. Transfections were conducted on Neuro-2A, PC12 cells or mature cortical neurons using pFlag-IKK-2 (IKKβ Addgene #11103), IKKβ-directed small-hairpin RNA plasmids that were purchased from Origene (Rockville, MD, USA, TG509787'A'-'D') or pAnkG-eGFP (270 kDa; a kind gift from V. Bennett, Duke University Medical Center, Durham, NC, USA), AnkG shRNA (Konig et al., 2012) as well as an eGFP vector. PC12 cells were transfected with NF-κB-response element firefly luciferase (pGL4.32[luc2P/NF-κB-RE/Hygro] vector (Promega, Southampton, UK, Cat#E8491) or NF-κB-luciferase (P. Baeuerle, Freiburg, Germany) and phRL-TK Renilla-luciferase expressing construct under constitutive thymidine-kinase promoter control (Promega, Cat#E6241) at a ratio of 14:1 for normalization in Dual-Luciferase assays (Promega) that were conducted using manufacturer's recommendations.

4.3 Molecular cloning of death-domain deficient ankyrin-G vectors (pAnkG-ΔDD) and the death-domain of ankyrin-G (DD of ankyrin-eGFP). For the generation of death-domain excised ankyrin-G vectors, we first digested 270kDa eGFP-N1-ankyrin-G using *ApaI* and column purified the linearized vector. Following double-digestion using *EcoRV* and *XbaI*, and subsequent to alkaline phosphatase (Fermentas) treatment, we re-ligated the long fragment back with the eGFP comprising C-terminal fragment following gel purification. We used the following primers to amplify the death domain of ankyrin-G from rat total DNA preparations: 5'ATGCAAGCTTGCCACCATGGTCCACATCGAAAAAGGTCCAC-3' and 5'-ATGCGGATCCATGGTGCCTGAAATATTCCCATAATC-3' which where inserted into EGFP-N1 following *HindIII* and *BamHI* digestion.

4.4 Animal Procedures. Animal procedures were carried out under a license from the Department of Health and Children of Ireland (B100/3688) and the Health

Products Regulatory authority (HPRA, AE19127/P005), were compliant with EC Directive 86/609/EEC for animal experiments and were previously approved by the Research Ethics Committee of the Royal College of Surgeons in Ireland (REC131 & 817).

4.5 Immunofluorescence and flow cytometry analyses. Fixation of live neurons was performed immediately following media removal. Notably, prolonged (>1 min) pre-fixation incubation in ice-cold PBS resulted in notably diminished immunoreactivity using phosphorylation-specific antibodies. Glass-sealed formaldehyde solutions (Mallinkrodt, Dublin, Ireland) were freshly diluted from 16% to 3% content using 1 x cytoskeletal buffer (CB buffer: 10 mM PIPES (pH 6.8), 150 mM NaCl, 5 mM EGTA, 5 mM β-D-glucose, 5 mM $MgCl_2$) and brought to 37 ºC before addition to the wells. Where applicable, extraction of live cells was performed at 4 ºC for 5 minutes in 1% (m/V) Triton-X-100 in 10 mM Na_3PO_4-buffer (pH 7.4), 1 mM $MgCl_2$, 3 mM $CaCl_2$, 150 mM NaCl. Solutions were pre-chilled before washes with cold PBS, and fixation. Cells were permeabilized following washes, using ice-cold HBSS containing 0.1% (w/v) Triton X-100, blocked for 30 minutes with 0.3% (w/v) Triton X-100 and 5% (v/v) HS in HBSS. They were incubated for 2 hours at room temperature or overnight at 4 ºC in primary antibody dissolved in 0.3% (w/v) Triton X-100, 1% (v/v) HS in HBSS. For the labeling of brain slices, mice were sacrificed with an overdose of pentobarbital and transcardially perfused with 2% (for the cortical slices) or 4% (for the cerebellar slices) paraformaldehyde in 0.1 M phosphate-buffered saline. Coronal vibratome slices were obtained (50 μm) and stained free-floating following blocking procedures. Brains from mice with a targeted deletion of the cerebellar form of ankyrin-G (Zhou et al., 1998) and their controls were stained following post-fixation overnight at 4 ºC. For immunofluorescence

analyses, we used the following antibodies: A mouse monoclonal anti-ankyrin-G (1:500, 463, Santa Cruz Biotechnology (scbt) Cat# sc-12719, RRID:AB_626674, Heidelberg, Germany), a rabbit polyclonal anti-(pan)-IKKα/β, (1:1000, H-470, scbt, Cat# sc-7607, RRID:AB_675667), a rabbit polyclonal anti-Ser177/Ser181-phosphorylated IKKα/β (pIKKα/β, 1:500, clone 16A6, Cell Signaling Technology (CST) Cat# 2697P, RRID:AB_10120863, Hitchin, UK), a rabbit polyclonal anti-Ser181-phosphorylated IKKα/β (pSer181-IKKα/β, 1:500, scbt, Cat# sc-23470, RRID:AB_331624), a goat polyclonal anti-Ser177/Ser181-phosphorylated IKKα/β (1:500, scbt, Cat# sc-23470-R, RRID:AB_2122159), a rabbit polyclonal anti-Thr183/Tyr185-phosphorylated SAPK/JNK antibody (1:500, CST, Cat# 9251, RRID:AB_331659), a rabbit polyclonal anti-Thr180/Tyr182-phosphorylated p38-MAPK antibody (1:500, CST, Cat# 9211, RRID:AB_331641), a rabbit polyclonal and a mouse monclonal anti-Ser536-phosphorylated p65 antibody (1:500, 93H1, CST, Cat# 4025S, RRID:AB_10827881 & 7F1, CST, Cat# 3036S, RRID:AB_331281), a mouse monoclonal phospho-S32/36-IκBα antibody (1:500, CST, Cat# 9246L, RRID:AB_2267145), and anti-calbindin (Swant, Bellinzona, Switzerland). Following three washes in ice-cold HBSS, cultures were incubated for 1 hour at RT with secondary antibodies raised against the appropriate species bearing tags with either Alexa–Fluor-488 or -568 (Gibco-Invitrogen). Photomicrographs were obtained using a SPOT RT SE 6 Camera (Diagnostic Instruments, Sterling Heights, USA) or an Eclipse TE 300 inverted microscope (Nikon, Kinston upon Thames, UK) with Mercury-arc light bulbs. A Zeiss 510 or 710 LSM (Carl Zeiss, Jena, Germany) was used for confocal image analyses. Co-localization analyses were performed using CoLocalizer Express® software (CoLocalizer research software, Japan&Switzerland) and ImageJ (NIH, Bethesda, MD, USA) using the 'colocalisation test' plug-in with

Costes approximation. Correlation of anti-phorphorylated IKK immunoreactivity with that against ankyrin-G was conducted in Matlab (Mathworks, Galway, Ireland). For Fluorescence-activated cell sorting (FACS) analysis on a BD-LSRII (BD Medical, Dun Laoghaire, Ireland), PC12 cells were transfected using Lipofectamine 2000. Two days following transfection, pre-warmed 2% formaldehyde in CB-buffer was applied for fixation. The reaction was quenched using 100 mM glycine in PBS (50%) and HBSS (50%), then spun at 2000 rpm for 5 minutes. Labelling was performed overnight with anti-pIKKα/β (1:500, CST) and anti-GFP (1:1000, B2, scbt, Cat# sc-9996, RRID:AB_627695) and anti-ankyrin-G (1:1000, scbt) and respective secondary antibody labelling. Experiments were run using two laser intensity settings. For detection, the following settings were used, FSC:450, SSC:270: eGFP (excitation 488/emission 525±25), Alexa-568 (561/605±20).

4.6 Proximity-ligation assays. Proximity-ligation assays were conducted on formaldehyde-fixed primary cortical neurons. Briefly, following standard immunofluorescence procedures including primary antibody incubation (rabbit anti-phospho-IKKα/β (1:500, CST), mouse anti-IKKβ (1:500, Abcam, Cat# ab52775, RRID:AB_881558) or rabbit anti-IKKα/β (1:500, CST), and or with mouse monoclonal anti-ankyrin-G (1:500, scbt, were used overnight), incubation of Olink-specific plus/minus oligonucleotide-linked antibodies in antibody-dilution buffer followed (Duolink, Olink Bioscience, Uppsala, Sweden). Hybridisation of oligonucleotides and detection was conducted as advised in the manufacturer's instructions, washes were performed with HBSS solutions.

4.7 Western-blot. For Western-blot analyses cells were lysed in RIPA buffer (150 mM NaCl, 1.0% IGEPAL CA-630, 0.5% sodium-deoxycholate, 0.1% sodium dodecyl sulphate, 50 mM Tris-HCl, pH 8.0, including protease and phosphatase

inhibitor cocktail). Following standard procedures for cell lysis and protein determination, equal amounts of proteins were separated by 8-15% gel electrophoresis as appropriate and blotted using semi-dry transfer (Biorad, Hercules, CA, USA). Following blocking procedures in 3-5% milk-TBS and 0.05% Tween-20, phosphorylation-specific antibodies were dissolved in Tris-buffered saline, 0.05% Tween-20, while 3% milk was included for pan-specific antibodies. The following antibodies were used in Western blotting, mouse monoclonal anti-ankyrin-G (1:1000, scbt), rabbit polyclonal anti-phospho-S536-p65 (1:500, CST), anti-pan-p65 (1:5000, F-6X, scbt, Cat# sc-8008, RRID:AB_628017), rabbit anti-IKKα/β (1:1000, H-470, scbt), rabbit polyclonal anti-pIKKα/β (1:500, CST), a rabbit polyclonal anti-pIκBα (1:500, CST, Cat# 5209S, RRID:AB_10829358), mouse monoclonal anti-α-Tubulin (dm1a, 1:5000, Sigma-Aldrich, Cat# T9026, RRID:AB_477593) and mouse monoclonal anti-GAPDH (1:1000, 6C5, Abcam, Cat# ab92412, RRID:AB_2278693). Detection was performed by incubation with the appropriate HRP-linked secondary antibody (Jackson Immunoresearch, Newmarket, UK).

4.8 Statistical analysis. We employed GraphPad Prism for statistical analyses (GraphPad Software Inc., La Jolla, USA). Parametric testing was performed and we conducted staticstical analyses as detailed in the figure legends. All data are represented as mean ± S.E.M., unless stated otherwise. p values ≤ 0.05 were considered to be significantly different and marked by an asterisk.

Acknowledgments: The authors would like to thank Christian Schultz, Mannheim, Germany for tissue derived from cerebellar-specific ankyrin-G knock-out mice, originally generated in the group of Vann Bennett (Duke University Medical Center, Durham, NC, USA), whom we also thank for the kind provision of the 270 kDa ankyrinG-eGFP construct. Further, the authors would like to thank Ina Woods for technical assistance; Jasmin Schmid for generation of the correlation plot in MatLab; Dr. Heiko Düssmann for his help with confocal microscopy and Dr. Christian Hellwig for his assistance with the fluorescence-assisted cell sorter.

Funding:

This work was supported by Science Foundation Ireland [08/IN.1/B1949; 14/IA/2582] and the European Union [EU FP7-EpiMiRNA under agreement Nr. 602130]. The authors declare that they have no conflict of interest.

References.

Baranauskas, G., David, Y., Fleidervish, I.A., 2013. Spatial mismatch between the Na+ flux and spike initiation in axon initial segment. Proc Natl Acad Sci U S A. 110, 4051-6.

Beg, A.A., et al., 1995. Constitutive NF-kappa B activation, enhanced granulopoiesis, and neonatal lethality in I kappa B alpha-deficient mice. Genes Dev. 9, 2736-46.

Bender, K.J., Trussell, L.O., 2009. Axon initial segment Ca2+ channels influence action potential generation and timing. Neuron. 61, 259-71.

Brachet, A., et al., 2010. Ankyrin G restricts ion channel diffusion at the axonal initial segment before the establishment of the diffusion barrier. J Cell Biol. 191, 383-95.

Buffington, S.A., et al., 2012. IkappaBalpha is not required for axon initial segment assembly. Mol Cell Neurosci. 50, 1-9.

Bui, N.T., et al., 2001. Activation of nuclear factor kappaB and Bcl-x survival gene expression by nerve growth factor requires tyrosine phosphorylation of IkappaBalpha. J Cell Biol. 152, 753-64.

Burke, J.R., et al., 2003. BMS-345541 is a highly selective inhibitor of I kappa B kinase that binds at an allosteric site of the enzyme and blocks NF-kappa B-dependent transcription in mice. J Biol Chem. 278, 1450-6.

Cavalli, V., et al., 2005. Sunday Driver links axonal transport to damage signaling. J Cell Biol. 168, 775-87.

Chen, Z., et al., 1995. Signal-induced site-specific phosphorylation targets I kappa B alpha to the ubiquitin-proteasome pathway. Genes Dev. 9, 1586-97.

Del Rio, M., et al., 2004. The death domain of kidney ankyrin interacts with Fas and promotes Fas-mediated cell death in renal epithelia. J Am Soc Nephrol. 15, 41-51.

Emmanouil, M., et al., 2009. Neuronal I kappa B kinase beta protects mice from autoimmune encephalomyelitis by mediating neuroprotective and immunosuppressive effects in the central nervous system. J Immunol. 183, 7877-89.

Feldman, M., Cryer, B., 1999. Aspirin absorption rates and platelet inhibition times with 325-mg buffered aspirin tablets (chewed or swallowed intact) and with buffered aspirin solution. Am J Cardiol. 84, 404-9.

Freal, A., et al., 2016. Cooperative Interactions between 480 kDa Ankyrin-G and EB Proteins Assemble the Axon Initial Segment. J Neurosci. 36, 4421-33.

Gasser, A., et al., 2012. An ankyrinG-binding motif is necessary and sufficient for targeting Nav1.6 sodium channels to axon initial segments and nodes of Ranvier. J Neurosci. 32, 7232-43.

Gaudreault, P., Temple, A.R., Lovejoy, F.H., Jr., 1982. The relative severity of acute versus chronic salicylate poisoning in children: a clinical comparison. Pediatrics. 70, 566-9.

Gerdts, J., et al., 2011. Image-based screening identifies novel roles for IkappaB kinase and glycogen synthase kinase 3 in axonal degeneration. J Biol Chem. 286, 28011-8.

Goetze, B., et al., 2003. Coupling the iron-responsive element to GFP--an inducible system to study translation in a single living cell. Sci STKE. 2003, PL12.

Grilli, M., et al., 1996. Neuroprotection by aspirin and sodium salicylate through blockade of NF-kappaB activation. Science. 274, 1383-5.

Kaltschmidt, C., et al., 1994. Constitutive NF-kappa B activity in neurons. Mol Cell Biol. 14, 3981-92.

Kole, M.H., et al., 2008. Action potential generation requires a high sodium channel density in the axon initial segment. Nat Neurosci. 11, 178-86.

Konig, H.G., et al., 2012. Fibroblast growth factor homologous factor 1 interacts with NEMO to regulate NF-kappaB signaling in neurons. J Cell Sci. 125, 6058-70.

Konig, H.G., et al., 2017. NF-kappaB regulates neuronal ankyrin-G via a negative feedback loop. Sci Rep. 7, 42006.

Kretschmer, T., et al., 2004. Elevated ankyrin G in a plexiform neurofibroma and neuromas associated with pain. J Clin Neurosci. 11, 886-9.

Lavrik, I., Golks, A., Krammer, P.H., 2005. Death receptor signaling. J Cell Sci. 118, 265-7.

Lou, J.Y., et al., 2005. Fibroblast growth factor 14 is an intracellular modulator of voltage-gated sodium channels. J Physiol. 569, 179-93.

Meffert, M.K., et al., 2003. NF-kappa B functions in synaptic signaling and behavior. Nat Neurosci. 6, 1072-8.

Mercurio, F., et al., 1997. IKK-1 and IKK-2: cytokine-activated IkappaB kinases essential for NF-kappaB activation. Science. 278, 860-6.

Politi, C., et al., 2008. Accumulation of phosphorylated I kappaB alpha and activated IKK in nodes of Ranvier. Neuropathol Appl Neurobiol. 34, 357-65.

Pradere, J.P., et al., 2016. Negative regulation of NF-kappaB p65 activity by serine 536 phosphorylation. Sci Signal. 9, ra85.

Rasmussen, H.B., et al., 2007. Requirement of subunit co-assembly and ankyrin-G for M-channel localization at the axon initial segment. J Cell Sci. 120, 953-63.

Sakurai, H., et al., 2003. Tumor necrosis factor-alpha-induced IKK phosphorylation of NF-kappaB p65 on serine 536 is mediated through the TRAF2, TRAF5, and TAK1 signaling pathway. J Biol Chem. 278, 36916-23.

Sanchez-Ponce, D., et al., 2008. New role of IKK alpha/beta phosphorylated I kappa B alpha in axon outgrowth and axon initial segment development. Mol Cell Neurosci. 37, 832-44.

Schmeisser, M.J., et al., 2012. IkappaB kinase/nuclear factor kappaB-dependent insulin-like growth factor 2 (Igf2) expression regulates synapse formation and spine maturation via Igf2 receptor signaling. J Neurosci. 32, 5688-703.

Schultz, C., et al., 2006. Coincident enrichment of phosphorylated IkappaBalpha, activated IKK, and phosphorylated p65 in the axon initial segment of neurons. Mol Cell Neurosci. 33, 68-80.

Simpson, C.S., Morris, B.J., 2000. Regulation of neuronal cell adhesion molecule expression by NF-kappa B. J Biol Chem. 275, 16879-84.

Soderberg, O., et al., 2007. Proximity ligation: a specific and versatile tool for the proteomic era. Genet Eng (N Y). 28, 85-93.

Strickson, S., et al., 2013. The anti-inflammatory drug BAY 11-7082 suppresses the MyD88-dependent signalling network by targeting the ubiquitin system. Biochem J. 451, 427-37.

Tarantino, N., et al., 2014. TNF and IL-1 exhibit distinct ubiquitin requirements for inducing NEMO-IKK supramolecular structures. J Cell Biol. 204, 231-45.

Wang, C., et al., 2001. TAK1 is a ubiquitin-dependent kinase of MKK and IKK. Nature. 412, 346-51.

Wildburger, N.C., et al., 2015. Quantitative proteomics reveals protein-protein interactions with fibroblast growth factor 12 as a component of the voltage-gated sodium channel 1.2 (nav1.2) macromolecular complex in Mammalian brain. Mol Cell Proteomics. 14, 1288-300.

Yang, J., et al., 2015. Pathological axonal death through a MAPK cascade that triggers a local energy deficit. Cell. 160, 161-76.

Yin, M.J., Yamamoto, Y., Gaynor, R.B., 1998. The anti-inflammatory agents aspirin and salicylate inhibit the activity of I(kappa)B kinase-beta. Nature. 396, 77-80.

Yu, P., et al., 2013. Global analysis of neuronal phosphoproteome regulation by chondroitin sulfate proteoglycans. PLoS One. 8, e59285.

Zandi, E., et al., 1997. The IkappaB kinase complex (IKK) contains two kinase subunits, IKKalpha and IKKbeta, necessary for IkappaB phosphorylation and NF-kappaB activation. Cell. 91, 243-52.

Zandi, E., Chen, Y., Karin, M., 1998. Direct phosphorylation of IkappaB by IKKalpha and IKKbeta: discrimination between free and NF-kappaB-bound substrate. Science. 281, 1360-3.

Zhang, X., Bennett, V., 1998. Restriction of 480/270-kD ankyrin G to axon proximal segments requires multiple ankyrin G-specific domains. J Cell Biol. 142, 1571-81.

Zhou, D., et al., 1998. AnkyrinG is required for clustering of voltage-gated Na channels at axon initial segments and for normal action potential firing. J Cell Biol. 143, 1295-304.

Figure legends.

Figure 1: Phosphorylated Ser177/181- and Ser181-IKKα/β-directed antibodies decorate the AIS in molecular proximity to IKKα/β-specific antibodies. (**A,B**) Mature mouse cortical neurons were formaldehyde (3%) fixed at 37 °C for 12 minutes and first incubated with anti-phospho-Ser177/181-IKKα/β (red, A) or anti anti-phospho-Ser181-IKKα/β (red, B) and ankyrin-G (green) specific antibodies and then appropriate fluorescently tagged secondary antibodies. (**C**) Mature cortical neurons were fixed as above and exposed to anti-phospho-p38 MAPK-specific antibodies (red). A phospho-IκBα-directed antibody was used to highlight the AIS (5A5, green). (**D**) Mature cortical neurons were fixed as above and exposed to anti-phospho-JNK/SAPK specific antibodies (red), and co-labeled with anti-ankyrin-G (green). (**E,F**) Cytosolic proteins were extracted from cultured cortical neurons on DIV 18 using a triton-X-100 extraction protocol for 5 min on ice. Subsequent to rapid formaldehyde fixation, the cultures were immunolabeled with anti-phospho-Ser177/181-IKKα/β (red, E), or anti-phospho-SAPK/JNK (red, F), together with ankyrin-G specific antibodies (green). (**G-I**) Schematic cartoon and results of the proximity-ligation assay for verification of epitopes in close proximity. Fixed mature cortical neurons were exposed to rabbit and mouse-derived anti pan-IKKα/β together with anti-phospho-Ser177/181-IKKα/β specific antibodies, followed by appropriate secondary oligonucleotide-linked antibody incubation, hybridization and rolling circle amplification (red). Ankyrin-G-specific antibodies (green) were used to identify the AIS. Note the accumulation of PLA-dots in the ankyrin-G-specific area (arrows in H). For quantification, the proximal dendritic area was estimated by drawing a circle around the cell body with the radius of the AIS and the somatic area was estimated by

drawing a circle with a center in the nucleus with a radius equivalent to the distance to the beginning of the AIS (I, n=15-19 cells, Box and Whiskers plot ± Tukey range, Kruskal-Wallis test). Peptide sequences around phosphorylation sites are shown (A-D). Boxed areas highlight exemplary AIS'. Scale bars, 10 μm.

Figure 2: Small-hairpin-mediated RNA interference of IKKβ from mature neurons reduces anti-phosphorylated IKKα/β immunofluorescence intensity in the AIS. (**A,B**) Neuro-2A cells were transfected with an IKKβ expression plasmid (1st lane), four different IKKβ-specific ('A'-'D') or control shRNA constructs. The cells were cultured for four days, lysed in RIPA-buffer and subjected to Western-blot procedure. A representative Western-blot is depicted in (A), the optical density relative to loading control was determined from 2-4 silencing experiments in (B). (**C-D**) DIV6-9 primary cultured cortical neurons were transfected with either constructs 'A' or 'C' as used above, or their combination, and incubated for 4 days. Following formaldehyde fixation (3%) for 12 minutes, neurons were subjected to immunofluorescent labeling using anti-phospho-Ser177/181-IKKα/β (red). eGFP (green), co-expressed from the same plasmids is depicted for transfection control (C). Arrows highlight exemplary AIS'. Profile of pIKKα/β immunofluorescence intensities along the AIS (D; n = 225-239 cells per group).

Figure 3: Phosphorylated IKKα/β immunoreactivity colocalizes with ankyrin-G immunoreactivity in the AIS during development *in vitro* and *in vivo*. (**A-C**) Mouse cortical neurons were cultured for two weeks, fixed by paraformaldehyde (3%)

incubation for 12 minutes and immunolabeled using phospho-Ser177/181-IKKα/β (red) and ankyrin-G (green) specific antibodies and imaged using a confocal microscope (A&B). At higher magnification a dotted anti pIKKα/β immunoreactivity was detectable that co-localized with ankyrin-G immunoreactivity (Pearson's correlation coefficient R=0.8305 from 3 planes of a stack of confocal images, B). Immunoreactivity intensities of phospho-Ser177/181-IKKα/β and ankyrin-G were measured from the end of the soma along the AIS and graphed against each other following normalization to their starting point in the AIS, the distance from the soma was color-coded using Matlab (C, n = 38 AIS', Spearman correlation coefficient of mean curve = 0.97). (**D**) Cortical neurons were fixed on DIV4, 7, 14 and 18, and co-immunolabeled with anti-pIKKα/β and ankyrin-G antibodies. (**E**) A mouse was perfused with 3% paraformaldehyde, the brain removed and brain slices obtained. Following pepsin-treatment (Konig et al., 2012), the free-floating slices were co-immunolabeled using phospho-Ser177/181-IKKα/β and ankyrin-G-specific antibodies. Scale bars, 10 μm.

Figure 4: Phosphorylated IKKα/β immunoreactivity is in molecular proximity with ankyrin-G immunoreactivity in the AIS. (**A-D**) The schematic cartoon highlights the principle of the proximity-ligation assay using anti-ankyrinG (raised in mouse) and anti-pIKKα/β-(raised in rabbit) specific antibodies (A). Mature cultured mouse cortical neurons were paraformaldehyde fixed, and incubated with ankyrin-G and pIKKα/β–specific antibodies and PLA assays performed (red). Ankyrin-G specific immunofluorescence was additionally obtained by incubation with anti-mouse-Alexa488 (green, B). The boxed area was obtained at higher magnification and

shown in (C). For quantification, the somatic and proximal dendritic area was estimated by drawing a circle around the cell body with the radius of the AIS, the number of PLA-spots in the ankyrin-G positive AIS versus somato-dendritic PLA spots was determined. Omission of primary antibody in the reaction served as negative control (D, n=23-29 axons, Box and Whiskers plot ± Tukey range, t-test). (**E**) Phosphorylated-IKKα/β does not accumulate in the proximal axon (arrows) of ankyrin-G-deficient Purkinje cells. Cerebellar slices from ankyrin-G-deficient or wild-type mice were stained using calbindin- (green; to mark Purkinje-cells) and phospho-IKKα/β-specific (red) antibodies. Scale bars, 10 μm.

Figure 5: Phosphorylated IKKα/β immunoreactivity co-localizes to pIκBα and p-p65 immunoreactivity in the AIS. Phosphorylated IKKα/β and p-p65 levels are increased by ankyrin-G overexpression. (**A**) Mouse cortical neurons were fixed and immunofluorescence using phosphorylated IKKα/β (rabbit, green) and Ser536-phosphorylated p65/NF-κB (pp65, mouse, red) antibodies was obtained. (**B**) Mouse cortical neurons were fixed and immunofluorescence using phosphorylated IKKα/β (rabbit, scbt, red) and anti-phosphorylated IκBα (5A5, CST, mouse, red) was obtained. Boxed area magnified below highlight membranous (arrows, red) and cytosolic immunoreactivities (green). (**C**) Rat PC12 cells were transfected with increasing amounts of ankyrin-G-eGFP and/or a constant amount of an IKKβ expression vector, and lysates subjected to Western-blotting procedure following 3 days of expression. (**D**) Twenty-four hours following transfection, flow cytometry was performed on fixed PC12 cells. Cells were transfected using eGFP or eGFP&IKKβ (black) and AnkG-eGFP (red) or AnkG-eGFP&IKKβ and stained with

anti-pIKKα/β. GFP-positive (GFP^+) cells were gated and the AUC of pIKKα/β immunofluorescence intensities were determined (from n = 2 cultures each including controls with comparable results, GFP-fluorescence positive cells were gated from n = 8,400-10,000 cells based on background fluorescence from non-transfected controls). (**E**) Cortical neurons were transfected with eGFP and/or IKKβ and/or ankG-eGFP. Following expression for two days the neurons were fixed and immunolabeled with Ser536-phosphorylated p65-specific antibodies. Arrows highlight prominent pp65-AIS immunoreactivity. Scale bars, 10 μm. (**F**) Schematic drawings of the Ankyrin-G constructs used below, M=membrane-binding domain, SP=Spectrin-binding domain, SR=Serine-rich domain, T=tail, DD=Death-domain (adapted from (Zhang and Bennett, 1998)). (**G**) PC12 cells were transfected with a small-hairpin RNA transcribing vector directed at ankyrin-G or a small-hairpin control vector together with a NF-κB response element (NF-κB-RE) reactive firefly luciferase reporter vector and a constitutive renilla-luciferase vector as transfection control. Mann-Whitney test, *p=0.0079, n=4 cultures from one plating. (**H**) PC12 cells were transfected with an eGFP vector or ankyrin-G eGFP together with the NF-κB-RE dual-luciferase vectors for one day. n=4 cultures from one plating. (**I**) PC12 cells were transfected with an eGFP vector, ankyrin-G-eGFP, ankyrin-G-eGFP deficient in the death-domain (ΔDD) together with the NF-κB dual-luciferase vectors, respectively. n=3 experiments. (**J**) PC12 cells were transfected with eGFP or a vector containing the death-domain of ankyrin-G linked to eGFP together with the NF-κB dual luciferase vectors. n=4 cultures from one plating. 1 value removed following ROUT outlier detection, n=4. (F-I) Dual-luciferase assays were conducted following cell lysis in passive lysis buffer on day one.

Figure 6. IKK-inhibitors deplete AIS-phospho-IKKα/β immunofluorescence. (**A,B**) Mature cortical neurons were incubated with distinct inhibitors of the IKK-complex or upstream signaling. BMS-345541, Bay11-7082, IKK-inhibitor VII or manumycin were added to the culture media at three different concentrations for 2 hours (n = 31-242 neurons pooled from 1-3 wells and 3-6 fields of view/treatment, Kruskal-Wallis test, Dunn's *post-hoc*, scale bars 10 µm). (**C**) Mature cortical neurons were incubated with two concentrations of acetylsalicylic acid (ASA) for twenty-four hours and the relative normalized immunofluorescence intensities of phosphorylated IKKα/β determined and plotted along the AIS. **(D)** Quantification of the single trace immunofluorescence intensities as determined in 'C' and depicted as AUC (6-17 axon traces, 'Box and Whiskers with Tukey range', Kruskal-Wallis test, Dunn's *post-hoc*, p=0.026).

Figure 1

Click here to download Figure: Figure1.pdf

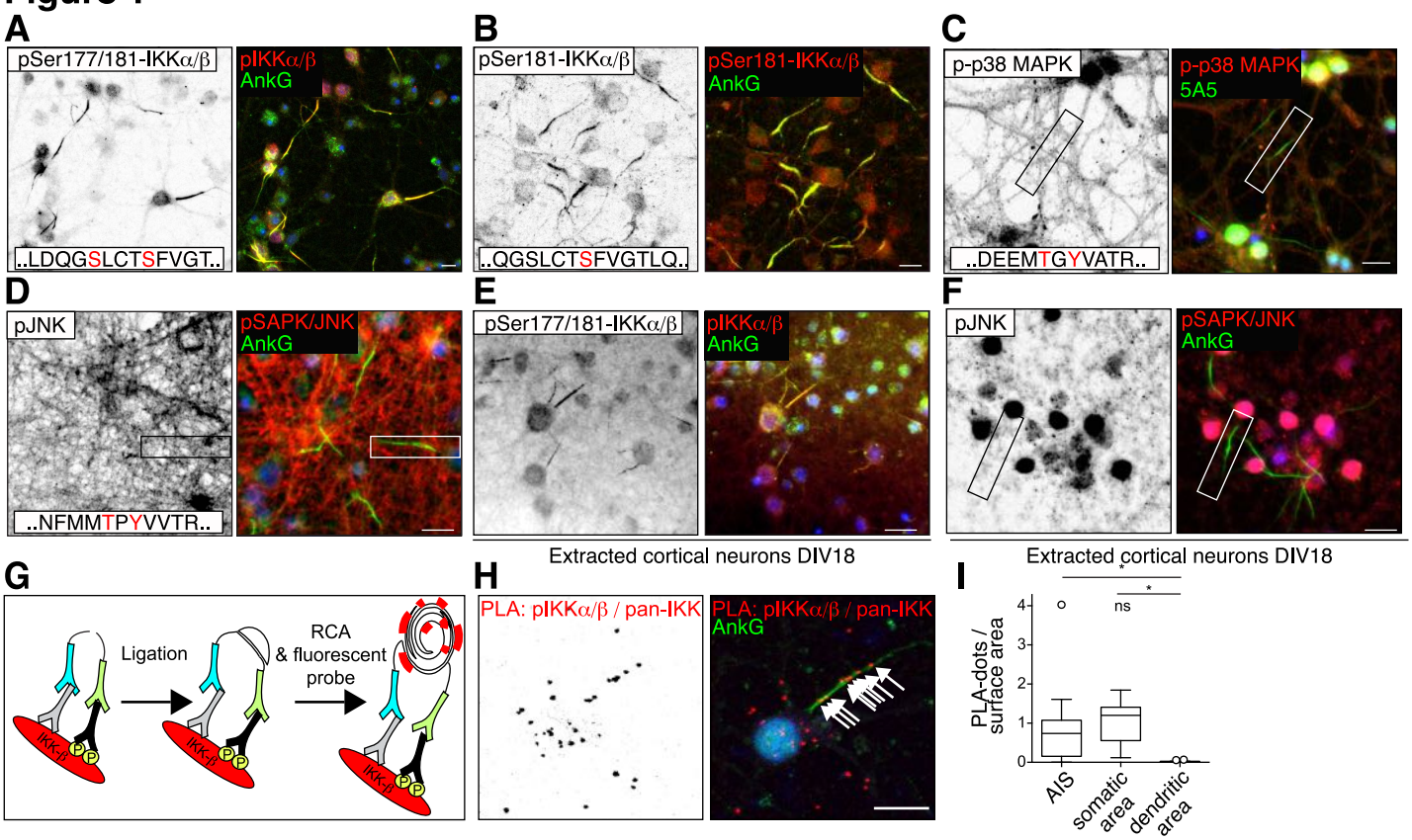

Figure 2

Click here to download Figure: Figure2.pdf

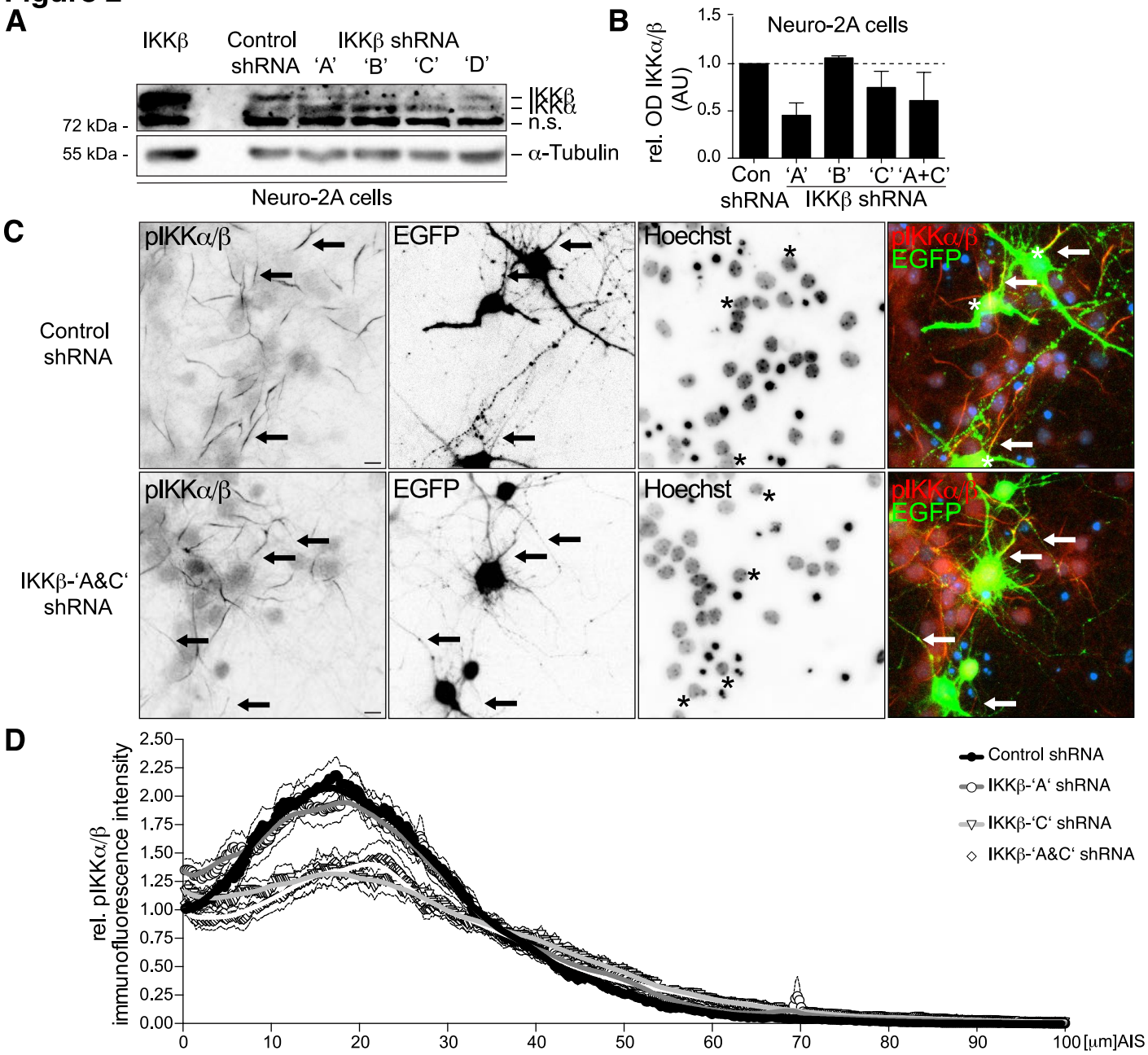

Figure 3

Click here to download Figure: Figure3.pdf

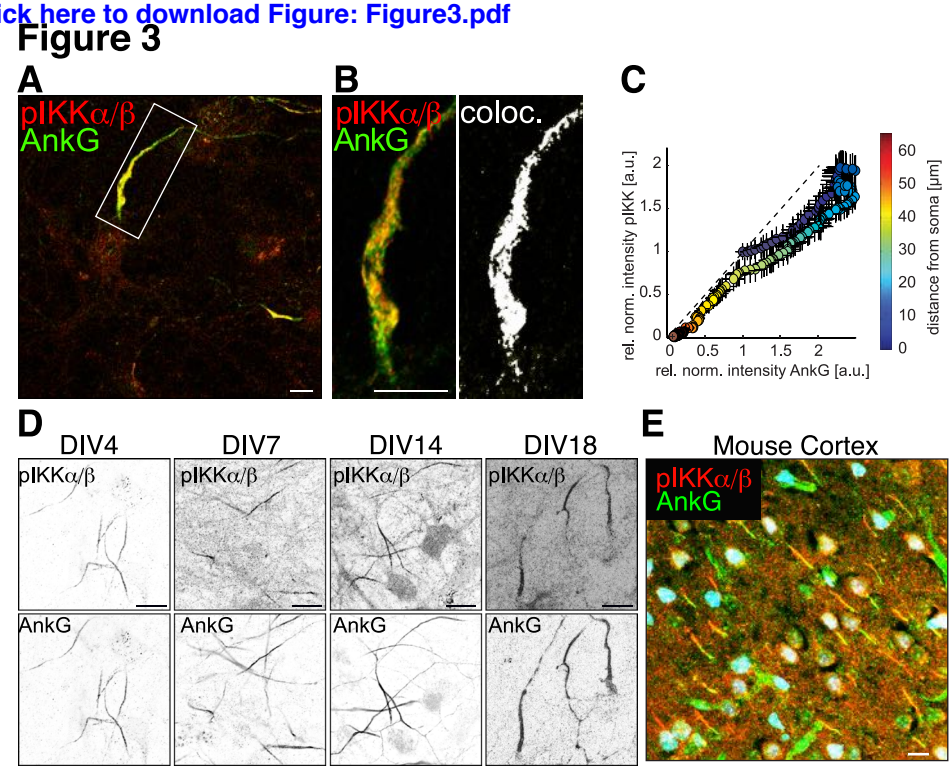

Figure 4

Click here to download Figure: Figure4.pdf

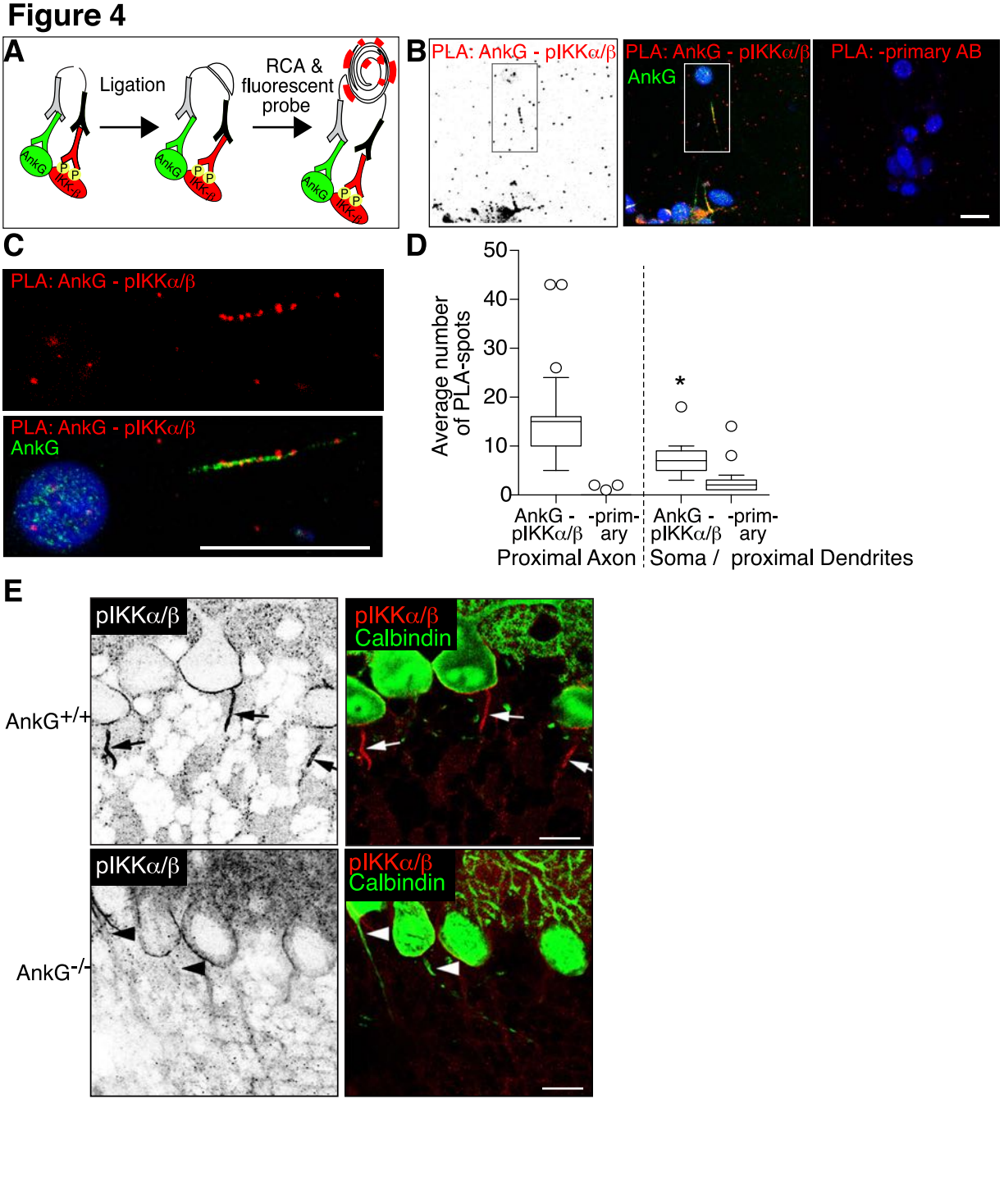

Figure 5

Click here to download Figure: Figure5.pdf

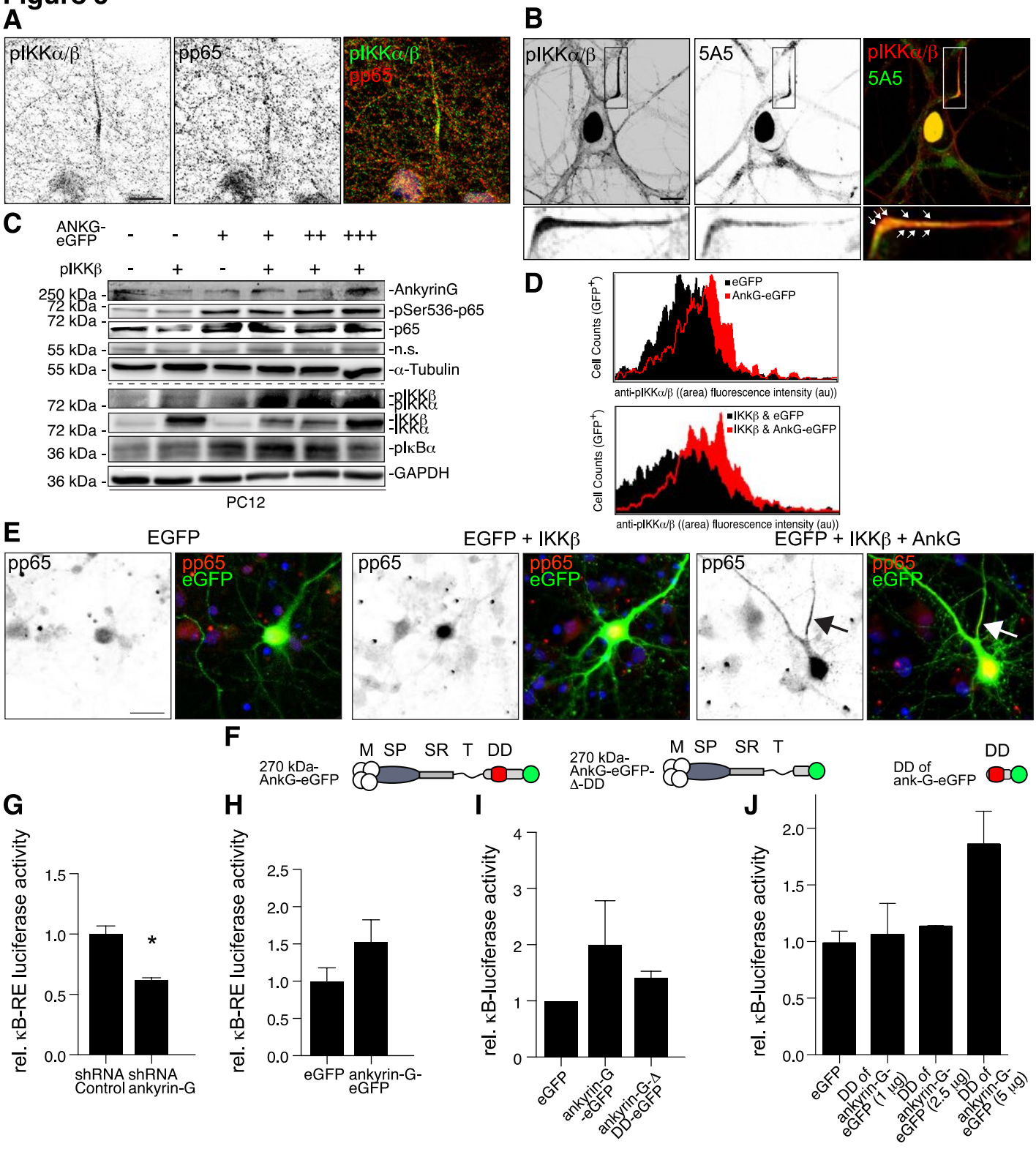

Figure 6

Click here to download Figure: Figure6.pdf

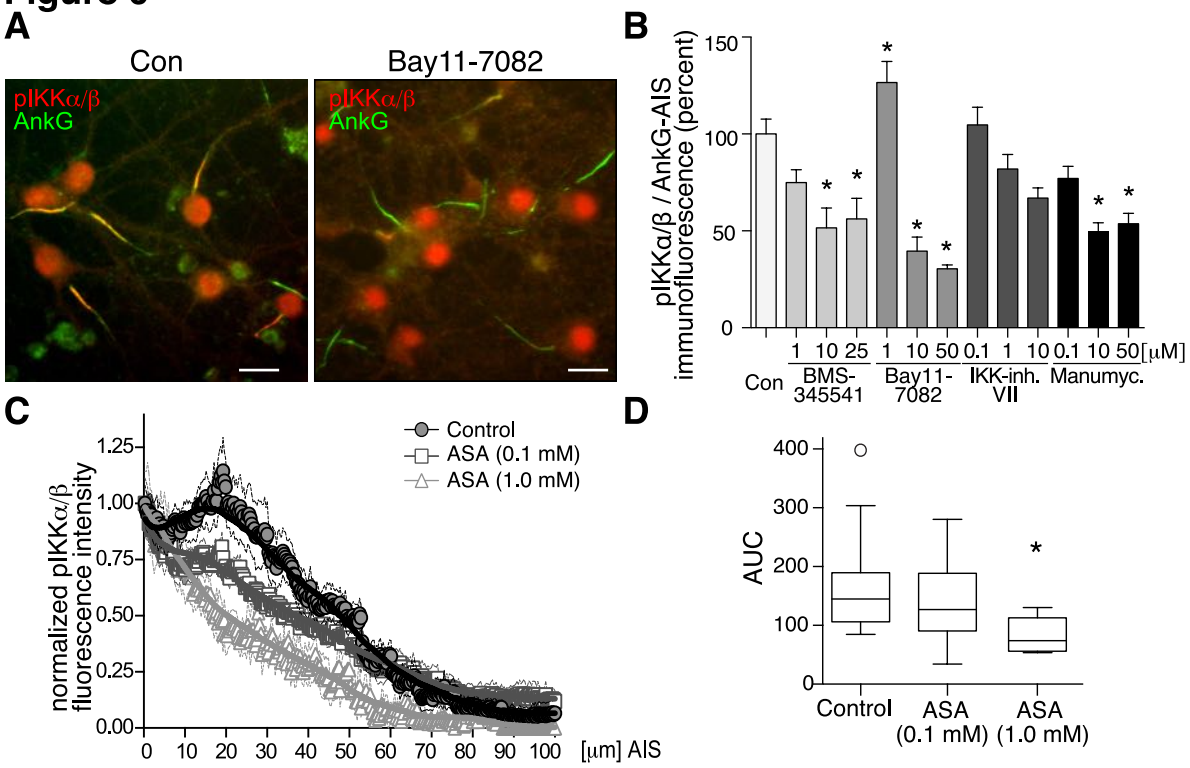

Graphical Abstract